

Lightning NO₂ simulation over the Contiguous US and its effects on satellite NO₂ retrievals

Response to Editor

Qindan Zhu, Joshua L. Laughner and Ronald C. Cohen

August 22, 2019

We thank the editor for very careful reading of both the main article and the supplement. Below we respond to the individual comments. The reviewer's comments will be shown in red, our response in blue, and changes made to the paper are shown in black block quotes. Unless otherwise indicated, page and line numbers correspond to the original paper. Figures, tables, or equations referenced as “Rn” are numbered within this response; Figures, tables, and equations numbered normally refer to the numbers in the original discussion paper.

In Figure 3, is the cloud fraction threshold of 0.2 used as in Figure 4? If so, please add this information to the caption

The cloud fraction threshold of 0.2 is also used in Figure 4. We modified the caption of Figure 4:

“Relative change in BEHR NO₂ VCD over the southeastern US switching the source of a prior NO₂ profiles from WRF-chem outputs using G3/CTH to one using KF/CAPE-PR lightning parameterization. (a) shows the mean spatial distribution of the changes from Aug 01 to Sep 23, 2013 and (b) shows the temporal variation over urban and rural areas. **Only observations with cloud fraction less than 20% are included.** Medium to large cities, including Atlanta, GA; Huntsville, AL; Birmingham, AL; Tallahassee, FL; Orlando, FL; and Baton Rouge, LA, are marked by stars in panel (a).”

On page 10, line 2, you cite Laughner et al., 2019 for the statement that “uncertainty due to AMF calculation for BEHR v3.0B is smaller than 30%. I couldn't find the corresponding statement in that paper and think that more qualification is needed? which parts of the uncertainty do you consider in this number? The way this number is used suggests that you exclude uncertainty from the vertical profile used? Why is it OK to assume that AMF uncertainties (which are strongly related to knowledge of surface reflection) are reduced like a random uncertainty when averaging?

The uncertainty evaluation of BEHR v3.0B is in the Section 6 of supplementary from Laughner et al. (2019). Summarized in Table S4 from Laughner et al. (2019), the uncertainty in AMF due to surface reflectance, surface pressure, tropopause pressure, cloud pressure,

cloud radiance fraction, and a priori profiles is determined by perturbing each parameter and re-retrieving the NO₂ VCD with the perturbed values. The calculated AMF uncertainty is less than 30% except for the winter.

Note that the uncertainty from the vertical profile is also included in the estimated AMF uncertainty. By improving the lightning parameterization in the models, we expect the uncertainty from the vertical profiles is lower than the previous calculation. The uncertainty in AMF of 30% is a very conservative estimate.

According to Figure S12 in Laughner et al. (2019), the a priori profile is the largest contributor to the AMF uncertainty, and tropopause pressure and cloud pressure are the next two largest contributors. Given that the uncertainty due to surface reflection is very small in general (<4%), we can treat daily AMF and VCD as independent variables and calculate the uncertainty due to AMF calculation as random uncertainty. We add the following text to point out the sources of uncertainty:

“We follow the same algorithm used in Laughner and Cohen (2017) to determine if the result is significant. The overall uncertainty due to AMF calculation for BEHR v3.0B is smaller than 30% during the study period (Sec 6 in supplementary from Laughner et al. (2019)). **Over 90% of the uncertainty attributes to the a priori NO₂ profiles, the tropopause and cloud pressures.** As each grid in Fig. 3(a) is the average of 45±9 pixels, the reduced uncertainty is less than 4.5%.”

In order to better understand the reason for the large changes over urban areas when changing the lightning parametrization it would be good to add figures showing vertical profiles of NO₂ for the three cases of no lightning, old parametrization and new parametrization as well as the scattering weights for the two cases of August 24 and September 10 that you discuss

We add Fig. S3 (also labeled as Fig. R1 in this response) in the supplementary. Note that we did not include the NO₂ profiles from WRF-Chem without lightning NO_x emissions, which are similar to the NO₂ profiles from WRF-Chem using KF/CAPE-PR with little NO₂ in the middle and upper troposphere over both urban and rural areas. For both days, switching from G3/CTH to KF/CAPE-PR parameterization in WRF-Chem substantially lowers the NO₂ in the upper troposphere. The difference in the relative change of VCD between two days is mainly due to the sensitivity in AMF to the erroneous high peak of NO₂ caused by G3/CTH parameterization in the middle and upper troposphere. We expand the discussion of the VCD changes on Sep 10 and Aug 24:

“Table 2 presents the AMF and VCD obtained from using a priori profiles with G3/CTH or KF/CAPE-PR lightning parameterizations as well as the relative changes on Sep 10 and Aug 24, 2013. **The corresponding a priori NO₂ profiles and scattering weights over urban and rural areas are shown in Fig. S3.** Sep 10 is an example of one day when the change in NO₂ profiles has a very large impact on the NO₂ VCDs. **The WRF-Chem using G3/CTH parameterization places a large amount of NO₂ between 200-600 hPa with the maximum value comparable to the near surface NO₂ over the**

urban areas. The calculated AMF is predominantly determined by lightning NO_2 due to the combination of higher scattering weight and larger NO_2 in the middle and upper troposphere. The change in AMF is -56.0% over urban areas and -32.0% over rural areas; the corresponding VCD increases by 134.9% and 44.9%, respectively. In contrast, Aug 24 is an example where the lightning parameterization has very little effect. **While the positive bias in NO_2 aloft is also observed by using G3/CTH parameterization, the amount of NO_2 in the middle and upper troposphere is smaller than Sep 10. It leads to lower sensitivity in AMF to the erroneous NO_2 caused by the lightning parameterization. With smaller relative change in AMF, the relative change in VCD is 3.1% over urban areas and -4.6% over rural areas. ”**

Please change the labels in Fig. 4 from “change in” to “difference in”
The figure is modified accordingly.

Please check again if the figures really show BEHR-WRF-Chem as stated in the text and in the caption. Judging from the numbers, I would guess that in fact WRF-Chem - BEHR is shown.

The figure shows WRF-Chem minus BEHR. We add it into the caption:

“Difference in NO_2 VCD between BEHR retrievals and WRF-Chem (“**WRF-Chem**” – “**BEHR**”). (a) excludes LNO_x in model simulation, (b) adds LNO_x emission with production rate of 500 mol NO flash⁻¹. (c) includes the same LNO_x emission as (b) but uses NO_2 profiles scaled upward by 60% at pressure lower than 400 hPa. The average time covers May 13 to June 23, 2012. Pixels with cloud fraction larger than 0.2 are filtered out in the analysis.”

Why is the spatial pattern of lightning (Fig. 1d) not reflected in Figure 4a?

Figure 1 and 4 average the datasets during the same study period. However, Fig 1 shows the daily lightning density over the US domain, whereas Fig 4 shows the NO_2 VCD at the OMI overpass time (~1:30 pm local time). Only lightning occurring before OMI overpass time contributes to the observed NO_2 VCD. We add it in Sec 2.4:

“The Ozone Monitoring Instrument (OMI) is an ultraviolet/visible (UV/Vis) nadir solar backscatter spectrometer launched in July 2004 on board the Aura satellite. It detects backscattered radiance in the range of 270-500 nm and the spectra are used to derive column NO_2 at a spatial resolution of 13 km×24 km at nadir (Levelt et al., 2006). **The OMI overpass time is ~13:30 local time.**”

References

Laughner, J. L. and Cohen, R. C.: Quantification of the effect of modeled lightning NO_2 on UV-visible air mass factors, Atmospheric Measurement Techniques, 10, 4403–4419, doi:

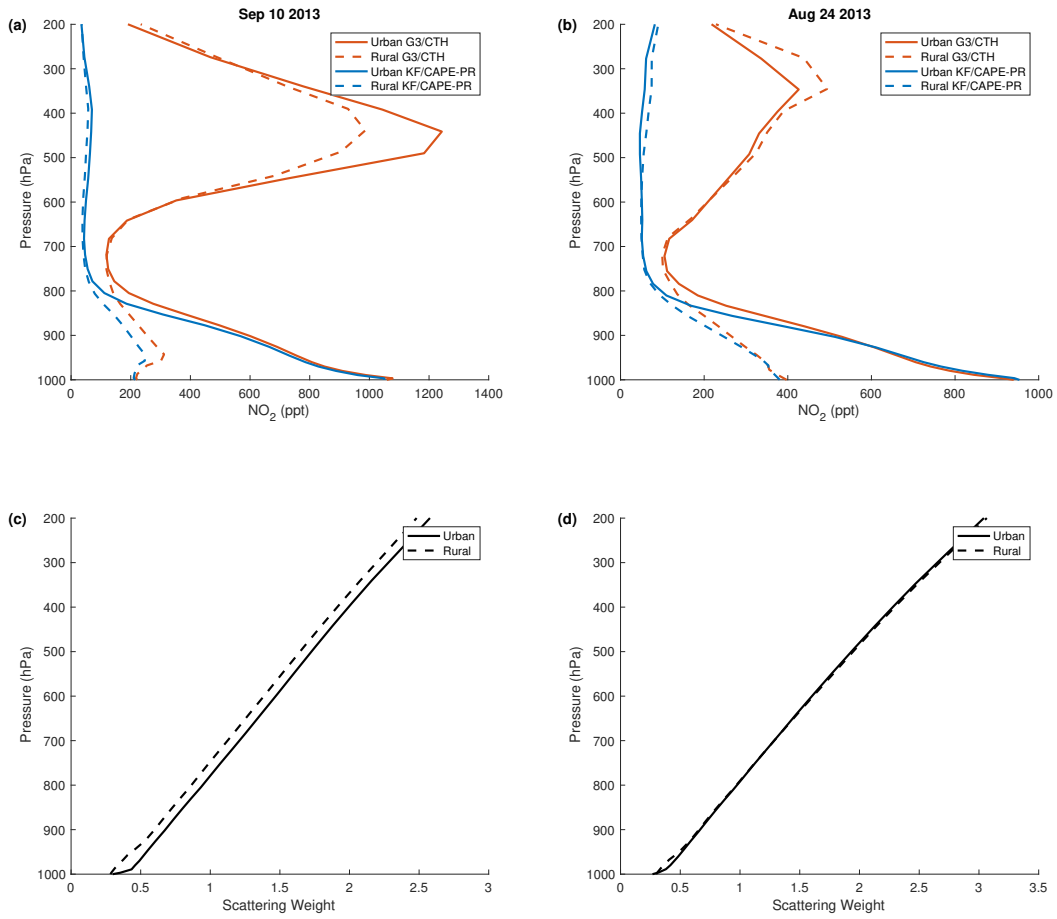


Figure R1: The a priori NO₂ vertical profiles (a, b) and scattering weights (c, d) on Sep 10 and Aug 24 2013 over all urban (solid) or rural (dashed) grid cells in SE US. The NO₂ profiles from WRF-Chem using G3/CTH parameterization are in red, those from KF/CAPE-PR parameterization are in blue.

10.5194/amt-10-4403-2017, URL <https://www.atmos-meas-tech.net/10/4403/2017/>, 2017.

Laughner, J. L., Zhu, Q., and Cohen, R. C.: Evaluation of version 3.0B of the BEHR OMI NO₂ product, *Atmospheric Measurement Techniques*, 12, 129–146, doi:10.5194/amt-12-129-2019, URL <https://www.atmos-meas-tech.net/12/129/2019/>, 2019.

Levelt, P., Oord, G., R. Dobber, M., Mlkki, A., Visser, H., Vries, J., Stammes, P., Lundell, J., and Saari, H.: The Ozone Monitoring Instrument, *IEEE T. Geoscience and Remote Sensing*, 44, 1093–1101, doi:10.1109/TGRS.2006.872333, 2006.

Lightning NO₂ simulation over the Contiguous US and its effects on satellite NO₂ retrievals

Response to Anonymous Referee #1

Qindan Zhu, Joshua L. Laughner and Ronald C. Cohen

August 22, 2019

We thank the reviewer for the positive response of the main article. Below we respond to the individual comments. The reviewer’s comments will be shown in red, our response in blue, and changes made to the paper are shown in black block quotes. Unless otherwise indicated, page and line numbers correspond to the original paper. Figures, tables, or equations referenced as “Rn” are numbered within this response; Figures, tables, and equations numbered normally refer to the numbers in the original discussion paper.

The abstract, the results, and the conclusions need to be enhanced to indicate the relative amounts of improvement due to changing convective schemes and changing lightning schemes. Table 1 shows that in the southeastern US just changing from G3 to KF produces the bulk of the improvement in slope and R2. With the KF scheme, changing from CTH to CAPE-PR only makes a small incremental improvement in slope and R2. Elsewhere, the change from G3/CTH to KF/CTH makes a 50% greater improvement in R2 than changing from KF/CTH to KF/CAPE-PR. So, the bottom line is that the convective scheme was more important than lightning scheme in yielding improved lightning prediction. The paper needs to say this.

Thanks for the suggestion. We modify the abstract to:

“Lightning is an important NO_x source representing ~10% of the global source of odd N and a much larger percentage in the upper troposphere. The poor understanding of spatial and temporal patterns of lightning contributes to a large uncertainty in understanding upper tropospheric chemistry. **We implement a lightning parameterization using the product of convective available potential energy (CAPE) and convective precipitation rate (PR) coupled with Kain Fritsch convective scheme (KF/CAPE-PR) into Weather Research and Forecasting-Chemistry (WRF-Chem) model. Compared to the cloud top height (CTH) lightning parameterization combined with Grell 3D convective scheme (G3/CTH), we show that the switch of convective scheme improves the correlation of lightning flash density in the southeastern US from 0.30 to 0.67 when comparing against the Earth Networks Total Lightning Network; the switch**

of lightning parameterization contributes to the improvement on correlation from 0.48 to 0.62 elsewhere in the US. The simulated NO₂ profiles using the KF/CAPE-PR parameterization exhibit better agreement with aircraft observations in the middle and upper troposphere.....”

In the Section 3.1, we rewrite the discussion on the comparison between modeled and observed lightning flash densities:

“Both models using the KF/CTH and KF/CAPE-PR parameterizations improves the correlation between modeled and observed lightning flash densities over the US domain. In the southeastern US, changing from G3 to KF convective scheme substantially increases the R^2 from 0.30 to 0.67 and reduces the slope from 2.08 to 0.94. Switching from CTH to CAPE-PR lightning parameterization only contributes a slight increment on the correlation. While the slopes close to unity both for KF/CTH and KF/CAPE-PR, we note that the improved scaling of the slope in KF/CAPE-PR is mainly caused by the scaling factor of 0.5 applied to the southeast region. In this simulation, a constant linear coefficient for CAPE-PR is not adequate to represent the observed lightning over CONUS, in contrast to the finding of Romps et al. (2014). Elsewhere in CONUS, both the changes in convective scheme and lightning parameterization yield a better representation of lightning flash densities compared to the observation. The R^2 for KF/CAPE-PR improves significantly to 0.62 compared to both G3/CTH and KF/CTH. The slope for KF/CAPE-PR is 1.19, which is within the uncertainty of the detection efficiency of ENTLN. In general the KF/CAPE-PR lightning parameterization captures the day-to-day variation in flash densities better than the G3/CTH and KF/CTH parameterizations as shown by the improved R^2 values.”

The conclusion is also modified accordingly:

“We implement an alternative lightning parameterization based on convective available potential energy and precipitation rate into WRF-Chem and couple it with Kain Frisch convective scheme. **We first validate it by comparing against lightning observations and find that the switch of convective scheme reproduces day-to-day variation of lightning flashes in the southeastern US and the switch of lightning parameterization contributes to the improvement on lightning representation elsewhere in the US.** We also compare the simulated NO₂ profiles against aircraft measurements and find that the simulated NO₂ using KF/CAPE-PR is more consistent with observations in the mid and upper troposphere.”

References

Romps, D. M., Seeley, J. T., Vollaro, D., and Molinari, J.: Projected increase in lightning strikes in the United States due to global warming, *Science*, 346, 851–854, doi:10.1126/science.1259100, URL <http://science.sciencemag.org/content/346/6211/851>, 2014.

Lightning NO₂ simulation over the Contiguous US and its effects on satellite NO₂ retrievals

Response to Anonymous Referee #2

Qindan Zhu, Joshua L. Laughner and Ronald C. Cohen

August 22, 2019

We thank the reviewer for the positive response of both the main article and the supplement. Below we respond to the individual comments. The reviewer's comments will be shown in red, our response in blue, and changes made to the paper are shown in black block quotes. Unless otherwise indicated, page and line numbers correspond to the original paper. Figures, tables, or equations referenced as “Rn” are numbered within this response; Figures, tables, and equations numbered normally refer to the numbers in the original discussion paper.

(1) The reason that I suggest deleting the statement? The model-satellite NO₂ column comparison suggests 500 mol NO flash⁻¹ is too high for the estimate of lightning NO_x production rate, but demonstrates that the uncertainty in the modeled UT [NO₂]/[NO_x] ratio is a key limiting factor in constraining production efficiency over CONUS in the far-field approaches in the conclusion section is not because I think far-field observations are unimportant for constraining LNO_x. But how well we understand NO/NO₂ ratio in the upper troposphere (with or without fresh lightning) shouldn't be mixed with LNO_x constraints. Since most of NO_x is in form of NO, high-quality NO measurements are sufficient to constrain LNO_x using far-field measurements. Even if we understand and can simulate NO₂/NO_x ratios in the upper troposphere well, the fact is that NO₂ is lower than NO and is arguably more difficult to measure. This last statement of the paper is rather odd to me. So for a third time, I'd suggest either deleting this sentence or providing detailed discussion of the need and application of having both in situ NO and NO₂ measurements as constraints of LNO_x.

We agree with the reviewer that the error in [NO₂]/[NO_x] ratio is limited for constraining LNO_x if accurate NO measurement is available. Our statement is based on the fact that OMI only observes NO₂ columns from the space. We decide to delete the statement in the conclusion.

(2) FYI, the R values listed in Table 1 of Luo et al.'s work is for 5-min flash rate comparison between the observations and model results. The correlation values in this work are for daily rates. More averaging can substantially improve R values.

We recognize the difference in the time resolution of lightning datasets between Luo et al. (2017) and this study. The rough comparison of correlation coefficients between this study

and Luo et al. (2017) in my last response is inappropriate.

(3) The authors should add some general comments on the differences between G3 and GF schemes in WRF-Chem to (1) explain the differences in the resulting LNOx distributions and (2) compare with the MM5 differences found by Zhao et al. (2009).

We add it in Section 3.1:

“...The G3/CTH parameterization fails to reproduce the spatial pattern of flashes observed by ENTLN over the CONUS. Compared to the G3/CTH, the KF/CTH parameterization improves the spatial correlation in the southeast region of US and yields a lower amount of lightning flashes. It indicates that KF convective scheme produces smaller cumulus cloud top heights than G3 scheme by including entrainment and detrainment processes during the convection. The result is consistent with Zhao et al. (2009). The KF/CAPE-PR parameterization better captures the spatial distribution of flash densities both in the southeast region and elsewhere in CONUS.”

(4) I suggest adding more discussion details on the differences between ENTLN and NLDN flash rate observations. Some of the details are already in the response. The absolute counts of flash rates by LIS are also uncertain and it should be mentioned. Since the authors have ENTLN and NLDN datasets, doing a direct comparison with LIS data (accounting for detection efficiencies) would seem straightforward. Why is it not included in the paper?

Among three lightning observation datasets, NLDN only observes CG lightning; ENTLN and LIS measure the total lightning flashes but LIS couldn't distinguish IC and CG lightning types. As we use ENTLN as the lightning observation reference, we intend to evaluate it by comparing against LIS and NLDN. The former one is already included, here we add the comparison between ENTLN and NLDN into the supplementary:

“

1 Comparison between ENTLN and NLDN

While both NLDN and ENTLN have high detection efficiency (>90%) for CG flashes, we recognize that ENTLN observes more CG flashes than NLDN. Shown in Fig. R1, we average the flashes density over CONUS both from ENTLN and NLDN between May 13 to June 23 2012. The daily averaged CG flash density from ENTLN is tightly correlated with those from NLDN with slope of 1.5. It can be explained by discrepancy in the grouping criteria applied to produce flash counts between NLDN and ENTLN. ENTLN groups all pulses within 10 km and 700 ms of each other as a single flash, and NLDN uses 10 km and 1000 ms as the threshold. In consequence, for the same amount of CG pulses measured by both lightning observation network, ENTLN produces more flashes than NLDN according to the grouping algorithm. ”

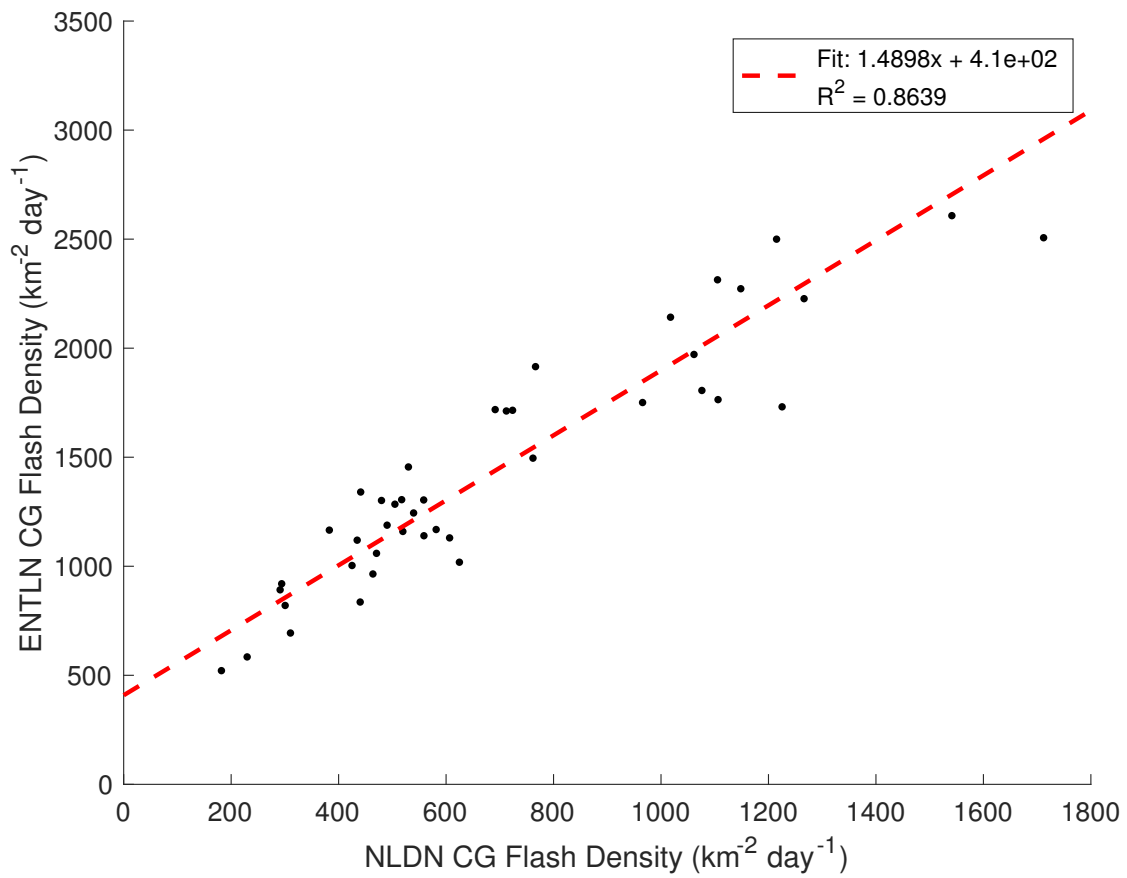


Figure R1: Comparison between CG flash density per day observed by NLDN and ENTLN. The data spans May 13 to June 23, 2012.

(5) In Figure 3, the large urban VCD change is not due to lightning over Orlando. What is the reason then? The authors don't have ENTLN data for that period, can they look at NLDN data to see how well the model simulates lightning flash distribution over urban regions? There are only 4 figures in this paper; adding more discussion cannot hurt.

Figure 3 shows the VCD changes by switching a priori profiles produced from WRF-Chem using G3/CTH to the one using KF/CAPE-PR. Since this is a model-model comparison the accuracy of the lightning observations is not especially useful. The area with large VCD difference is also much larger than Orlando from Fig 3 (a).

Besides, the VCD changes are not linear with lightning changes in the models. VCD is calculated by dividing SCD (slant column density) by AMF, and AMF is obtained based on scattering weights and a priori NO_2 profiles. We add a more detailed discussion on the AMF and VCD changes in the last paragraph of Sec 3.3:

“Table 2 presents the AMF and VCD obtained from using a priori profiles with G3/CTH or KF/CAPE-PR lightning parameterizations as well as the relative changes on Sep 10 and Aug 24, 2013. **The corresponding a priori NO_2 profiles and scattering weights over urban and rural areas are shown in Fig. S2.** Sep 10 is an example of one day when the change in NO_2 profiles has a very large impact on the NO_2 VCDs. **The WRF-Chem using G3/CTH parameterization places a large amount of NO_2 between 200-600 hPa with the maximum value comparable to the near surface NO_2 over the urban areas. The calculated AMF is predominantly determined by lightning NO_2 due to the combination of higher scattering weight and larger NO_2 in the middle and upper troposphere.** The change in AMF is -56.0% over urban areas and -32.0% over rural areas; the corresponding VCD increases by 134.9% and 44.9%, respectively. In contrast, Aug 24 is an example where the lightning parameterization has very little effect. **While the positive bias in NO_2 aloft is also observed by using G3/CTH parameterization, the amount of NO_2 in the middle and upper troposphere is smaller than Sep 10. It leads to lower sensitivity in AMF to the erroneous NO_2 caused by the lightning parameterization. With smaller relative change in AMF, the relative change in VCD is 3.1% over urban areas and -4.6% over rural areas.** ”

References

- Luo, C., Wang, Y., and Koshak, W. J.: Development of a self-consistent lightning NO_x simulation in large-scale 3-D models, *Journal of Geophysical Research: Atmospheres*, 122, 3141–3154, doi:10.1002/2016JD026225, URL <https://agupubs.onlinelibrary.wiley.com/doi/abs/10.1002/2016JD026225>, 2017.
- Zhao, C., Wang, Y., Choi, Y., and Zeng, T.: Summertime impact of convective transport and lightning NO_x production over North America: modeling dependence on meteorological simulations, *Atmospheric Chemistry and Physics*, 9, 4315–4327, doi:10.5194/acp-9-4315-2009, URL <https://www.atmos-chem-phys.net/9/4315/2009/>, 2009.

Lightning NO₂ simulation over the Contiguous US and its effects on satellite NO₂ retrievals

Qindan Zhu¹, Joshua L. Laughner^{2,*}, and Ronald C. Cohen^{1,2}

¹Department of Earth and Planetary Sciences, University of California, Berkeley, Berkeley, CA 94720

²Department of Chemistry, University of California, Berkeley, Berkeley, CA 94720

*Now in Department of Environmental Science and Engineering, California Institute of Technology, Pasadena, CA 91125

Correspondence: Ronald C. Cohen (rccohen@berkeley.edu)

Abstract. Lightning is an important NO_x source representing ~10% of the global source of odd N and a much larger percentage in the upper troposphere. The poor understanding of spatial and temporal patterns of lightning contributes to a large uncertainty in understanding upper tropospheric chemistry. We implement a lightning parameterization using the product of convective available potential energy (CAPE) and convective precipitation rate (PR) [coupled with Kain Fritsch convective scheme \(KF/CAPE-PR\)](#) into Weather Research and Forecasting-Chemistry (WRF-Chem) model. ~~The CAPE-PR parameterization with a regional scaling factor of 0.5 in the southeastern US, is coupled with Kain Fritsch~~ [Compared to the cloud top height \(CTH\) lightning parameterization combined with Grell 3D convective scheme \(KFG3/CAPE-PR\) to generate lightning for the continental US. We](#) ~~CTH), we~~ show that the ~~KF/CAPE-PR scheme yields an improved representation of lightning flashes in WRF~~ [switch of convective scheme improves the correlation of lightning flash density in the southeastern US from 0.30 to 0.67](#) when comparing against ~~flash density from~~ the Earth Networks Total Lightning Network. ~~Compared to the cloud top height (CTH) lightning parameterization coupled with Grell 3D convective scheme (G3/CTH) used in WRF-Chem,;~~ [the switch of lightning parameterization contributes to the improvement on correlation from 0.48 to 0.62 elsewhere in the US.](#) The simulated NO₂ profiles using the KF/CAPE-PR parameterization exhibit better agreement with aircraft observations in the middle and upper troposphere. Using a lightning NO_x production rate of 500 mol NO flash⁻¹, the a priori NO₂ profile generated by the simulation with the KF/CAPE-PR parameterization reduces the air mass factor for NO₂ retrievals by 16% on average in the southeastern US on the late spring and early summer compared to simulations using the G3/CTH parameterization. This causes an average change in NO₂ vertical column density four times higher than the average uncertainty.

1 Introduction

Nitrogen oxides (NO_x ≡ NO + NO₂) are key species in atmospheric chemistry, affecting the oxidative capacity in the troposphere by regulating the ozone and hydroxyl radical concentrations (Crutzen, 1979). Anthropogenic sources (mainly fossil fuel combustion) are the largest contributor to the NO_x budget on a global scale. Natural sources of NO_x are also nonnegligible (Denman et al., 2007). While anthropogenic emissions of NO_x are intensively studied, natural sources are less understood (e.g. Delmas et al., 1997; Lamsal et al., 2011; Miyazaki et al., 2012). Lightning contributes to ~10% of NO_x budget on a global scale and represents over 80% of NO_x in the upper troposphere (UT) (Schumann and Huntrieser, 2007; Nault et al., 2017). Over the

US, the anthropogenic NO_x emissions have been decreasing rapidly (Russell et al., 2012; Lu et al., 2015), making lightning an increasingly important source of NO_x and an increasingly large fraction of the source of column NO_2 . Ozone (O_3) in UT has long lifetime and leads to a more pronounced radiative effect than ozone elsewhere in the troposphere. Varying lightning NO_x emission (LNO_x) by a factor of four (123 to 492 mol NO flash⁻¹) yields up to 60 % enhancement of UT O_3 and increases the mean net radiative flux by a factor of three (Liaskos et al., 2015). This range in the lightning NO_x production rate is similar to the current uncertainty of estimated lightning emission rates. Further, incorrect representation of LNO_x in a priori profiles for satellite NO_2 retrievals leads to biases in the retrieved NO_2 columns. This is exacerbated by the greater sensitivity of UV/Vis NO_2 retrievals to the UT (e.g. Laughner and Cohen, 2017; Travis et al., 2016).

When lightning occurs, NO is emitted as a result of high temperatures and NO_2 forms through rapid photochemistry. Studies report the estimated LNO_x production rate ranges widely from 16 to 700 mol NO flash⁻¹ (DeCaria et al., 2005; Hudman et al., 2007; Martin et al., 2007; Schumann and Huntrieser, 2007; Huntrieser et al., 2009; Beirle et al., 2010; Bucsela et al., 2010; Jourdain et al., 2010; Ott et al., 2010; Miyazaki et al., 2014; Liaskos et al., 2015; Pickering et al., 2016; Pollack et al., 2016; Laughner and Cohen, 2017; Nault et al., 2017).

Two categories of methods, one emphasizing the near-field of lightning NO_x and the other the far-field, have previously been applied to estimate LNO_x . In near-field approaches the total NO_x from direct observation close to the lightning flashes is divided by the number of flashes from a lightning observation network to yield the NO_x per flash (e.g. Schumann and Huntrieser, 2007; Huntrieser et al., 2009; Pollack et al., 2016). Near-field estimates of LNO_x per flash have also been made through use of cloud-resolved models with LNO_x constrained by observed flashes and aircraft data from storm anvils (e.g. DeCaria et al., 2005; Ott et al., 2010; Cummings et al., 2013). In contrast, the far-field approach uses downwind observations to constrain a regional or global chemical transport model. The emission rate of lightning NO_x is varied in the model (either ad hoc or through formal assimilation methods) until the modeled NO_x agrees with the measurements of total NO_x at the far field location (Hudman et al., 2007; Martin et al., 2007; Jourdain et al., 2010; Miyazaki et al., 2014; Liaskos et al., 2015; Laughner and Cohen, 2017; Nault et al., 2017). In general, far-field approaches yield estimates of LNO_x at the upper end of reported range, while estimates from the near-field studies are typically at the lower end of the range. Nault et al. (2017) showed that a large part of this discrepancy is because prior near-field studies assume a long NO_x lifetime in the UT, while active peroxy radical chemistry in the near field leads to a short NO_x lifetime (~3 h). Without accounting for this chemical loss, the near-field and far-field estimates are biased low compared to each other. However, this effect cannot completely reconcile the discrepancy between LNO_x reported from near- and far- field studies.

In chemical transport models, LNO_x production is modeled by assuming a fixed number of moles of NO are produced per lightning flash, typically 250 or 500 mol NO flash⁻¹ (Zhao et al., 2009; Allen et al., 2010; Ott et al., 2010). This presents an additional challenge to the far-field approaches to constrain LNO_x , as errors in the simulation of lightning flashrate will propagate into errors in the LNO_x production per flash. However, explicitly simulating the cloud scale processes that produce lightning is generally too computationally expensive to be applied in a regional or global model as it requires spatial resolution at the scale of cloud processes. Instead, the convection is parameterized using simplified convection schemes. Lightning is then parameterized by a suite of convection parameters. The most prevalent lightning parameterization relates lightning to the

cloud top height (CTH) (Price and Rind, 1992; Price et al., 1997). Price and Rind found a consistent proportionality between cloud-to-ground (CG) lightning flashes and the fifth power of cloud top height. Other meteorological variables, including upward cloud mass flux (UMF), convective precipitation rate (CPR), convective available potential energy (CAPE), cloud ice flux (ICEFLUX) have been suggested as alternative lightning proxies for CG flashes or in some cases total flashes (Allen and
5 Pickering, 2002; Choi et al., 2005; Wong et al., 2013; Romps et al., 2014; Finney et al., 2014). When CG flashes are predicted, the total lightning rate, including CG and Intra-Cloud (IC) flashes, is derived by defining a regional dependent CG:IC ratio (Boccippio et al., 2002).

Several previous studies have evaluated the performance of these lightning parameterizations in regional and global models. Tost et al. (2007) concluded none of them accurately reproduce the observed lightning observations even though some are
10 inter-comparable. Wong et al. (2013) showed that a model using the Grell-Devenyi ensemble convective parameterization and the CTH lightning parameterization simulates erroneous flash count frequency distribution over time while the integrated lightning flash count is consistent with the observation. Luo et al. (2017) tested the single-variable parameterizations (CTH, CAPE, UMF, CPR) and the paired parameterizations based on power law relationship (CAPE-CTH, CAPE-UMF, UMF-CTH), each of which was coupled with Kain Frisch convective scheme, and demonstrated that the two-variable parameterization using
15 CAPE-CTH improves upon the previous single-variable parameterizations; it captures temporal change of flash rates but the simulated spatial distribution is still not satisfactory.

In this study, we implemented the CAPE-PR lightning parameterization (Romps et al., 2014) into WRF-Chem and assess the performance in reproducing lightning flash density. Our motivation is to produce a better representation of a proxy-based lightning parameterization in the regional chemistry transport model. We also evaluate the effect of modeled lightning NO_x on
20 both the a priori profiles used in satellite NO_2 retrievals and the retrievals themselves.

2 Methods: models and observations

2.1 WRF-Chem

This study applies the Weather Research and Forecast Model coupled with Chemistry (WRF-Chem) version 3.5.1 to the time periods May to June, 2012 and August to September, 2013. The model domain covers North America from 20°N to 50°N
25 with $12\text{ km} \times 12\text{ km}$ horizontal resolution and 29 vertical layers. The North American Regional Reanalysis (NARR) provides initial and boundary conditions. Temperature, wind direction, wind speed and water vapor are nudged every 3 h towards to NARR product. Chemistry initial and boundary conditions are provided by the Model for Ozone and Related Chemistry Tracers (MOZART, <https://www.acom.ucar.edu/wrf-chem/mozart.shtml>). Anthropogenic emissions are driven by the National Emissions Inventory 2011 (NEI 11), with a scaling factor to match the total emissions to 2012 emission from the Environmental
30 Protection Agency (EPA, 2016). Biogenic emissions are driven by the Model of Emissions of Gases and Aerosol from Nature (MEGAN; (Guenther et al., 2006)). We use a customized version of the Regional Atmospheric Chemistry Mechanism version 2 (RACM2), the details are described by Zare et al. (2018).

The default lightning parameterization used in WRF-Chem is based on cloud top height (CTH). The parameterized lightning flash rates are proportional to a power of cloud top height with linear scaling varied by region:

$$f = \begin{cases} 3.44 \times 10^{-5} H^{4.9} & \text{Continental} \\ 6.20 \times 10^{-4} H^{1.73} & \text{Marine} \end{cases} \quad (1)$$

5 where f is the CG flash rate in each grid and H is the colocated cloud top height in units of kilometers.

We also implement an alternative lightning parameterization where lightning flash rates are defined to be proportional to the product of the convective available potential energy (CAPE) and precipitation rate (PR).

$$f = \begin{cases} 0.9 \times 10^{-4} \times E \times PR & \text{Southeastern CONUS} \\ 1.8 \times 10^{-4} \times E \times PR & \text{Elsewhere CONUS} \end{cases} \quad (2)$$

where f the CG flash rate in each grid cell, E the convective available potential energy and PR the convective precipitation rate. Southeastern CONUS in the context is the region between 94 °W to 76 °W and 25 °N to 37 °N. This parameterization was proposed by Romps et al. (2014). Romps et al. (2014) used a year-round observation of lightning and meteorological parameters and found a good correlation between observed lightning flash densities and observed CAPE times PR over the CONUS. CAPE-PR was further examined in Tippett and Koshak (2018) who computed the proxy in a numerical forecast model and found a fairly good agreement between the spatial pattern of the daily CG flash rate and the forecast proxy over 15 2003-2016. To our knowledge CAPE-PR parameterization has not previously been coupled with chemistry. Note that we compute these two meteorological variables every 72 seconds in our model setup and produce lightning flash rates in a much shorter time step compared to Romps et al. (2014) and Tippett and Koshak (2018). We also apply a regional scaling factor of 0.5 to the southeastern US (See Sec 3.1).

We analyze WRF-Chem outputs from three model runs. The first run, referred as “G3/CTH”, is consistent with Laughner and Cohen (2017); it selects the Grell 3D ensemble cumulus convective scheme (Grell, 1993; Grell and Dévényi, 2002) and the CTH lightning parameterization. The Grell 3D convective scheme readily computes the neutral buoyancy level which serves as the optimal proxy for cloud top height (Wong et al., 2013). The “G3/CTH” is the only option for the coupled convective-lightning parameterization used in WRF-Chem at a non-cloud resolving resolution (12 km). In addition, we run WRF-Chem with the CTH lightning parameterization coupled with the Kain-Fritsch cumulus convective scheme (Kain and Fritsch, 1990; 25 Kain, 2004) (“KF/CTH”) to test the effect of switching convective schemes. In the “KF/CTH” parameterization, the cloud top height is the level where the updraft vertical velocity equals to zero. Another run, referred as “KF/CAPE-PR”, selects the Kain-Fritsch cumulus convective scheme and the CAPE-PR lightning parameterization described above. Compared to the Grell 3D convective scheme, the Kain-Fritsch uses the depletion of at least 90% CAPE as the closure assumption and calculates CAPE on the basis of entraining parcels instead of undiluted parcels, which also improves the calculation of precipitation rate (Kain, 30 2004). The lightning NO_x production rate is defined to be 500 mol NO flash⁻¹. The CG:IC ratio and the LNO_x post-convection vertical distribution are the same as used by Laughner and Cohen (2017).

2.2 ENTLN lightning observation network

To assess the performance of the lightning parameterizations we compare to lightning flashes from Earth Networks Total Lightning Network (ENTLN). ENTLN employs over 100 sensors across the United States and observes both CG and IC pulses
5 (<https://www.earthnetworks.com/why-us/networks/lightning/>). All lightning pulses within 10 km and 700 ms of each other are grouped as a single flash. The IC and CG flashes are summed over the grid spacing defined in WRF-Chem.

Compared to National Lightning Detection Network (NLDN), ENTLN is selected for high detection efficiencies of both CG and IC flashes. The average detection efficiency for total flashes observed by ENTLN was 88% over CONUS relative to the space-based Tropical Rainfall Measurement Mission (TRMM) Lightning Imaging Sensor (LIS) (Lapierre et al. (submitted),
10 private communication). Shown in Fig. S2, we matched the ENTLN data to LIS flashes both in time and space after the correction of LIS data based on its detection efficiency (Cecil et al., 2014) during May 13-June 23, 2012. It shows a median correlation ($R^2 = 0.51$) with the slope of 1.0, indicating the ENTLN data during the study time period is in agreement with the LIS observation. We use the ENTLN for analysis as reported and consider the detection efficiency of ENTLN as a source of uncertainty when comparing the modeled lightning flashes.

15 2.3 In Situ Aircraft Measurements

We compare our simulations to observations from aircraft campaigns that focus on deep convection. The Deep Convective Clouds and Chemistry (DC3) campaign (Barth et al., 2015) took place during May and June of 2012 over Colorado, Oklahoma, Texas and Alabama. The Studies of Emissions and Atmospheric Composition, Clouds, and Climate Coupling by Regional Surveys (SEAC4RS) (Toon et al., 2016) took place during August and September of 2013; most of the flight tracks occurred
20 over the southeastern US. Both aircraft campaigns flew into and out of storms and sampled deep convection. The combination of these two aircraft campaigns cover the regions with the most active lightning in the domain.

2.4 Satellite Measurements

The Ozone Monitoring Instrument ([OMI](#)) is an ultraviolet/visible (UV/Vis) nadir solar backscatter spectrometer launched in July 2004 on board the Aura satellite. It detects backscattered radiance in the range of 270-500 nm and the spectra are used to
25 derive column NO_2 at a spatial resolution of 13 km \times 24 km at nadir (Levelt et al., 2006). [The OMI overpass time is ~13:30 local time.](#)

We use the Berkeley High Resolution (BEHR) v3.0B OMI NO_2 retrieval (Laughner et al., 2018). The air mass factor (AMF) is calculated based on the high spatial resolution a priori input data including surface reflectance, surface elevation and NO_2 vertical profiles. In this study we apply an experimental branch of the BEHR product which differs from v3.0B in several ways.
30 First, instead of calculation based on temperature profiles from WRF-Chem, the tropopause pressure is switched to GEOS-5 monthly tropopause pressure which is consistent with NASA Standard Product (SP2) (Mak et al., 2018). Analysis shows the algorithm used in BEHR v3.0B to calculate the WRF-derived tropopause pressure is very much dependent on the vertical

| | | G3/CTH | KF/CTH | KF/CAPE-PR |
|--------------|-------|--------|--------|------------|
| Southeastern | Slope | 2.08 | 0.94 | 0.96 |
| | R^2 | 0.30 | 0.67 | 0.72 |
| Elsewhere | Slope | 0.98 | 0.54 | 1.19 |
| | R^2 | 0.27 | 0.48 | 0.62 |

Table 1. Correlation statistics between observed and modeled (G3/CTH, KF/CTH, KF/CAPE-PR) flash density per day averaged by regions

spacing predefined in WRF-Chem setup, which causes biases when the vertical layers are at a coarse resolution. Second, the NO_2 vertical profiles are outputs using the modified lightning parameterization described in Eq. 2.

3 Results

3.1 Comparison with observed lightning flash density

5 The lightning parameterizations are compared against observations from ENTLN in Fig 1. Each of the datasets is averaged from May 13 to June 23, 2012, covering DC3 field campaign. The ENTLN data is summed to the $12 \text{ km} \times 12 \text{ km}$ WRF grid. The G3/CTH parameterization fails to reproduce the spatial pattern of flashes observed by ENTLN over the CONUS. Compared to the G3/CTH, the KF/CTH parameterization improves the spatial correlation in the southeast region of US ~~-.The~~
10 ~~and yields a lower amount of lightning flashes. It indicates that KF convective scheme produces smaller cumulus cloud top heights than G3 scheme by including entrainment and detrainment processes during the convection. The result is consistent with Zhao et al. (2009). The~~ KF/CAPE-PR parameterization better captures the spatial distribution of flash densities both in the southeast region and elsewhere in CONUS. However the KF/CAPE-PR parameterization still fails to capture the gradients in flash occurrence within smaller regions. For instance, ENTLN shows that more lightning occurs along the east coast than west coast in Florida, however, WRF-Chem generates a lightning flash density of the same magnitude over both areas. Nevertheless,
15 the KF/CAPE-PR substantially improves the model performance in reproducing lightning spatial patterns.

To evaluate the agreement quantitatively, we regress the WRF daily regional average flash densities against those measured by ENTLN. The daily regional averaged flash density is calculated by summing the total flash rates and dividing them by the corresponding regional size. The regressions are shown in Fig 1 (e) and (f); the correlation statistics are shown in Table 1. The regressions by forcing intercept equals to zero are also tested, and the results are unaffected.

20 ~~The model Both models using the KF/CTH and KF/CAPE-PR lightning parameterization yields a tight correlation and slope close to the unity parameterizations improve the correlation between modeled and observed lightning flash densities over the US domain. In the southeastern US, changing from G3 to KF convective scheme substantially increases the R^2 increases from 0.3 to 0.7 and slope is reduced from 2.08 to 0.96 with the KF/0.94. Switching from CTH to CAPE-PR parameterization compared to the G3/CTH. The slope lightning parameterization only contributes a slight~~
25 ~~increment on the correlation. While the slopes close to unity both for KF/CTH is comparable to and KF/CAPE-PR while the~~

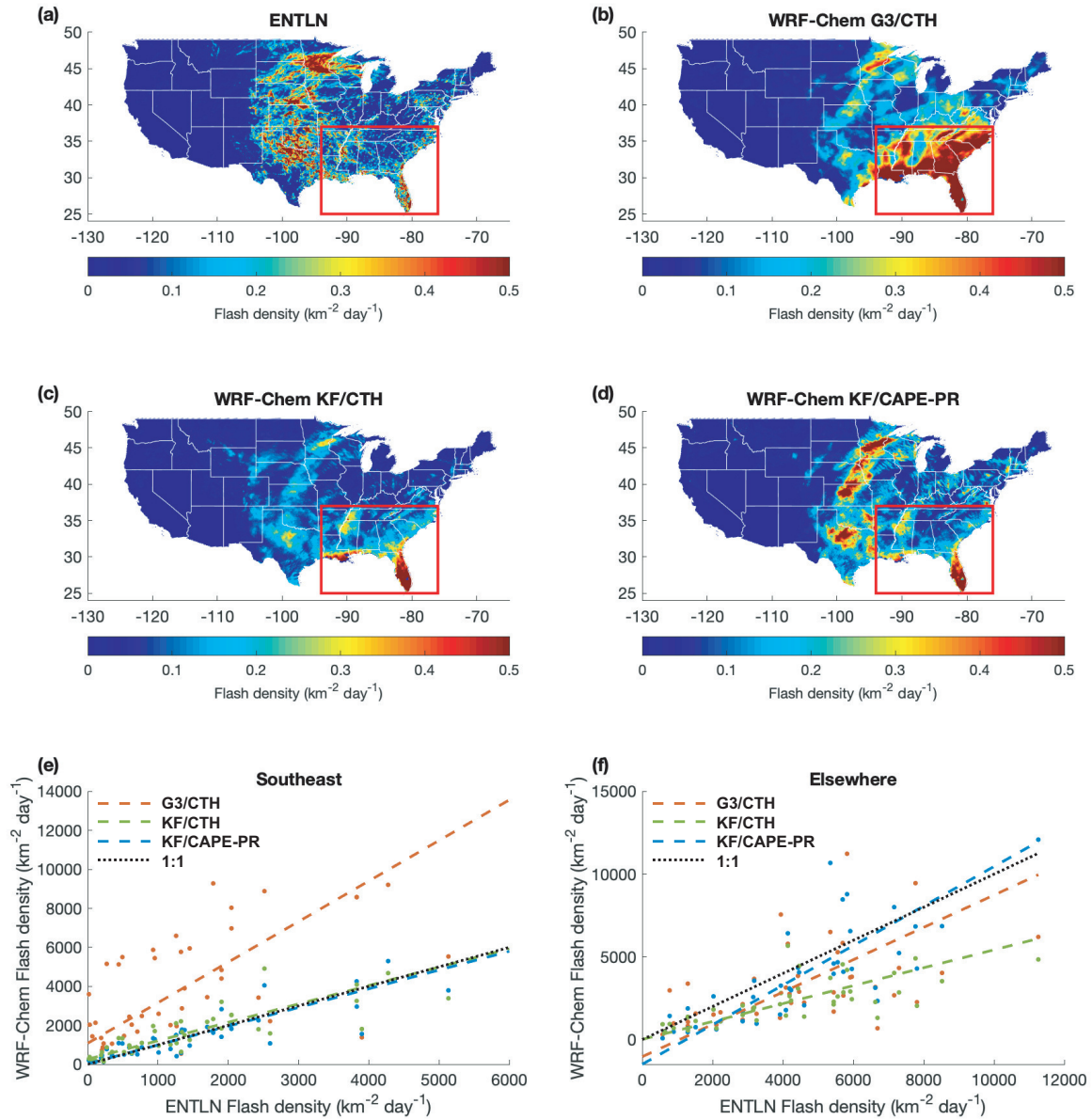


Figure 1. Observed flash densities from the ENTNLN dataset (a) and WRF-Chem using three coupled convective-lightning parameterizations, the G3/CTH parameterization (b), the KF/CTH parameterization (c) and the KF/CAPE-PR parameterization (d), respectively. The correlation of total flash density per day between WRF-Chem outputs and ENTNLN for the southeastern US (denoted by the red box in a-d) is shown in panel (e) and the correlation for elsewhere in CONUS is shown in (f). The model using G3/CTH is in red, KF/CTH is in green, and KF/CAPE-PR is in blue. Dash lines are corresponding fits. For slope and R^2 , see Table 1.

| | | AMF G3/CTH | AMF KF/CAPE-PR | % Δ AMF | VCD G3/CTH | VCD KF/CAPE-PR | % Δ VCD |
|--------|-------|------------|----------------|----------------|-----------------------|-----------------------|----------------|
| Sep 10 | Urban | 1.64 | 0.72 | -56.0 | 2.19×10^{15} | 5.16×10^{15} | 134.9 |
| | Rural | 1.96 | 1.33 | -32.0 | 1.11×10^{15} | 1.63×10^{15} | 44.9 |
| Aug 24 | Urban | 1.07 | 0.95 | -11.3 | 2.56×10^{15} | 2.64×10^{15} | 3.1 |
| | Rural | 1.23 | 1.25 | 1.60 | 1.91×10^{15} | 1.82×10^{15} | -4.6 |

Table 2. Differences for BEHR AMFs and tropospheric VCDs when using the a priori NO₂ profiles from models with CTH vs CAPE-PR parameterizations in the AMF calculation. For definitions of “urban” and “rural”, see the text.

~~R^2 for KF/CAPE-PR is slightly higher. Note, we note~~ that the improved scaling of the slope in KF/CAPE-PR is mainly caused by the scaling factor of 0.5 applied to the southeast region. In this simulation, a constant linear coefficient for CAPE-PR is not adequate to represent the observed lightning over CONUS, in contrast to the finding of Romps et al. (2014). Elsewhere in CONUS, ~~the both the changes in convective scheme and lightning parameterization yield a better representation of lightning flash densities compared to the observation. The~~ R^2 for KF/CAPE-PR improves significantly to ~~0.6-0.62~~ compared to both G3/CTH and KF/CTH. The slope for KF/CAPE-PR is 1.19, which is within the uncertainty of the detection efficiency of ENTLN. In general the KF/CAPE-PR lightning parameterization captures the day-to-day variation in flash densities better than the G3/CTH and KF/CTH parameterizations as shown by the improved R^2 values.

3.2 Comparison with observed vertical profiles

We compare the WRF NO₂ profile to the average vertical profile of NO₂ measured during DC3 and SEAC4RS in Fig 2. Data points are matched in time and space by finding the WRF-Chem output nearest in time and closest in space to a given observation. We only compare NO₂ profiles from WRF-Chem using KF/CAPE-PR against the one using G3/CTH.

The effect of lightning NO_x on the profiles is indistinguishable close to the surface. In the upper and middle troposphere, both model simulations yields similar NO₂ vertical profiles compared to the measurements from DC3. WRF-Chem using KF/CAPE-PR performs slightly better between 200 hPa to 400 hPa but the negative bias still exists. NO_x from both the observations and the models are very small in the middle troposphere between 400 hPa to 700 hPa.

Laughner et al. (2019) previously identified a high bias of WRF-Chem UT NO₂ versus SEAC4RS in the southeast US when using the G3/CTH parameterization. The model using the KF/CAPE-PR parameterization reduces this high bias of NO₂ in the middle and upper troposphere. The KF/CAPE-PR parameterization slightly overestimates NO₂ in the middle troposphere (400 - 530 hPa) and underestimates it in the upper troposphere (< 280 hPa), which is consistent with the comparison to observations from DC3 campaign.

3.3 Impact on BEHR NO₂ retrievals

In space-based retrievals of NO₂, the AMF is required to convert the slant column density (SCD) obtained by fitting the observed radiances into a vertical column density (VCD). The AMF depends on scattering weights (which describe the sensi-

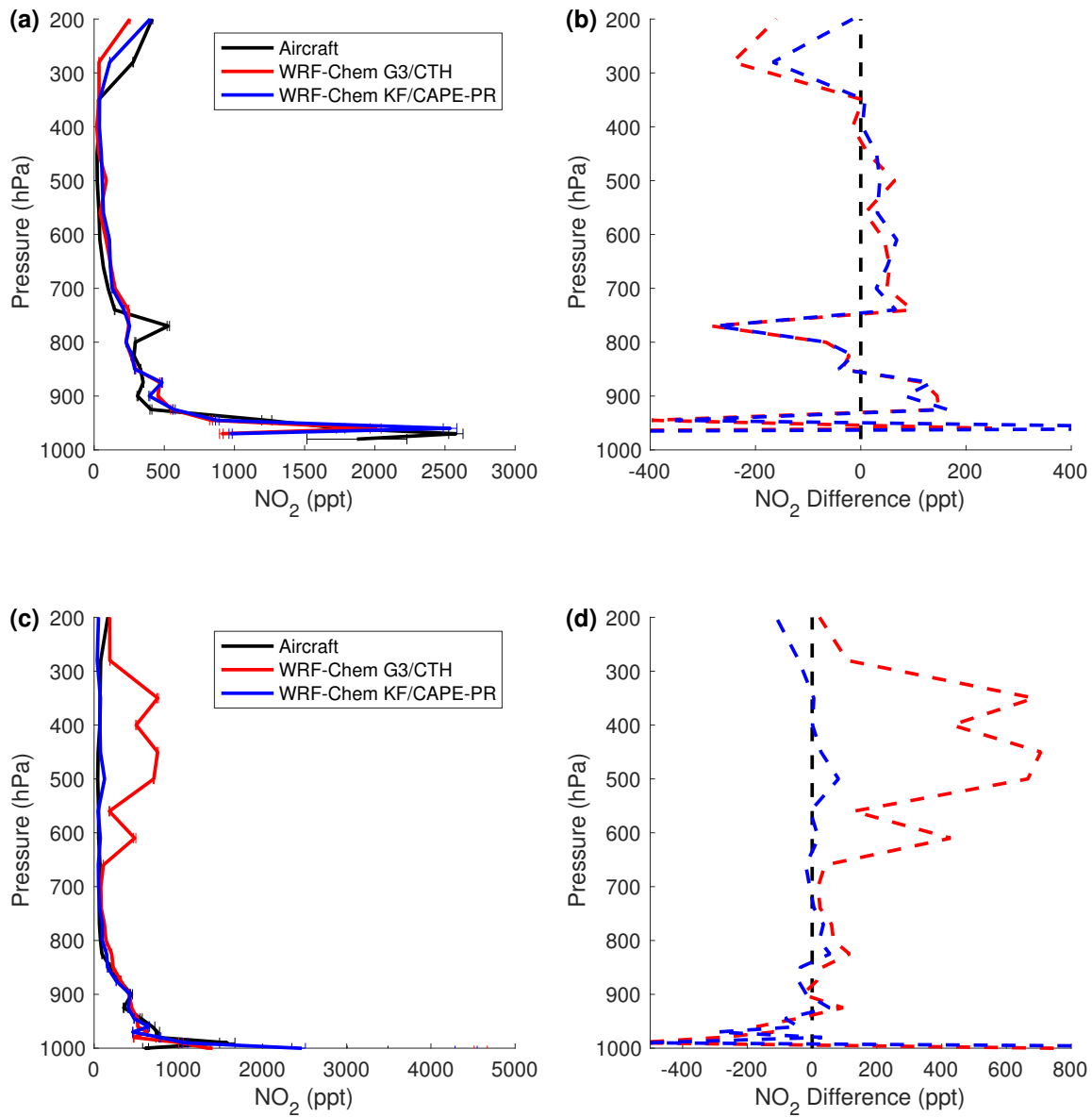


Figure 2. Comparison of WRF-Chem and aircraft NO₂ profiles from the (a,b) DC3, (c,d) SEAC4RS campaigns. Vertical NO₂ profiles are shown in (a,c), the solid line is the mean of all profiles and the bars are 1 standard deviation for each binned level. The corresponding absolute difference compared to observations are shown in (b,d). Aircraft measurements are shown in black, WRF-Chem using G3/CTH parameterization in red and WRF-Chem using KF/CAPE-PR parameterization in blue.

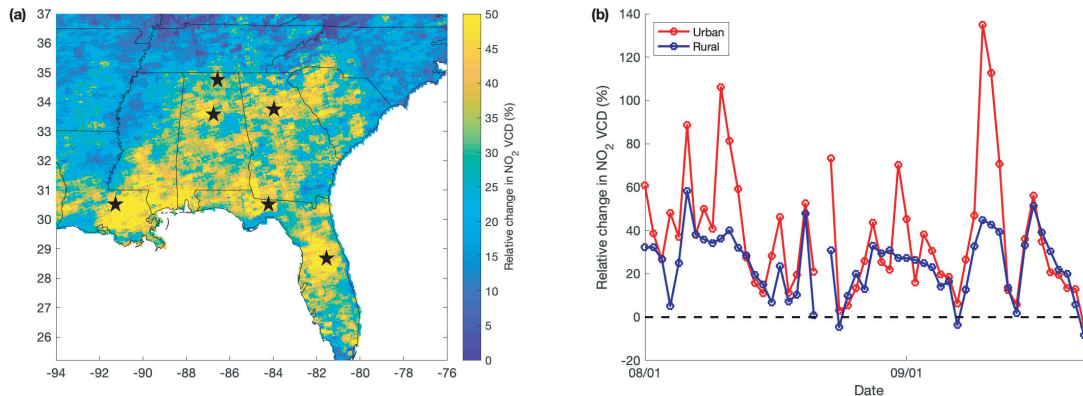


Figure 3. Relative change in BEHR NO_2 VCD over the southeastern US switching the source of a prior NO_2 profiles from WRF-chem outputs using G3/CTH to one using KF/CAPE-PR lightning parameterization. (a) shows the mean spatial distribution of the changes from Aug 01 to Sep 23, 2013 and (b) shows the temporal variation over urban and rural areas. Only observations with cloud fraction less than 20% are included. Medium to large cities, including Atlanta, GA; Huntsville, AL; Birmingham, AL; Tallahassee, FL; Orlando, FL; and Baton Rouge, LA, are marked by stars in panel (a).

tivity of the measurement to different levels of the atmosphere) and an NO_2 profile which is either measured or simulated by a chemical transport model, such as WRF-chem. Over a dark surface, the scattering weights in the UT are up to 10x greater than near the surface, due to the greater probability that a photon that reaches the lower troposphere will be absorbed by the surface. Therefore, errors in the UT NO_2 profile can have large effects on the AMF (e.g. Laughner and Cohen, 2017). Here, we investigate how the NO_2 profiles simulated by the KF/CAPE-PR parameterization affect the BEHR NO_2 retrievals.

5 Fig. 3(a) shows the relative change in tropospheric VCD averaged between Aug 01 to Sep 23, 2013 induced by changing the a priori profiles from the model using G3/CTH to the one using the KF/CAPE-PR lightning parameterization. The relative enhancement of VCD is 19% on average over southeast US but it varies significantly.

We follow the same algorithm used in Laughner and Cohen (2017) to determine if the result is significant. The overall uncertainty due to AMF calculation for BEHR v3.0B is smaller than 30% during the study period (Laughner et al., 2019).
 10 (Sec 6 in supplementary from Laughner et al. (2019)). Over 90% of the uncertainty attributes to the a priori NO_2 profiles, the tropopause and cloud pressures. As each grid in Fig. 3(a) is the average of 45 ± 9 pixels, the reduced uncertainty is less than 4.5%. The overall change in VCD is four times larger than the reduced uncertainty. The switch of lightning parameterization leads to changes in VCD exceeding the averaged uncertainty in ~94% of pixels in the southeast region of US.

The spatial pattern in Fig. 3(a) suggests that the magnitude of the improved representation of lightning is quite different in
 15 urban and rural areas. The cities indicated by stars and their vicinity regions are associated with substantial increase in NO_2 VCD. To quantify this, we define urban and rural areas by difference in column NO_2 calculated from WRF-Chem without LNO_x . Urban areas are the top 5% of columns with the average VCD of 2.2×10^{15} mole cm^{-2} . The selected rural areas have the same size as urban areas and the average VCD is 0.72×10^{15} mole cm^{-2} . Fig 3(b) shows the relative change in VCD

over the urban and rural areas as a function of time. The increase in VCD due to the change in profiles is more pronounced over urban areas with averaged relative change of ~38% compared to the average change of ~24% in rural areas. Changes in urban VCDs span -10% to 135%. In contrast, using the NO₂ profiles produced by the KF/CAPE-PR simulation leads to only maximum 58.3% increase in VCD over rural areas.

Table 2 presents the AMF and VCD obtained from using a priori profiles with G3/CTH or KF/CAPE-PR lightning parameterizations as well as the relative changes on Sep 10 and Aug 24, 2013. The corresponding a priori NO₂ profiles and scattering weights over urban and rural areas are shown in Fig. S3. Sep 10 is an example of one day when the change in NO₂ profiles has a very large impact on the NO₂ VCDs. The VCD increases by 134.9% WRF-Chem using G3/CTH parameterization places a large amount of NO₂ between 200-600 hPa with the maximum value comparable to the near surface NO₂ over the urban areas. The calculated AMF is predominantly determined by lightning NO₂ due to the combination of higher scattering weight and larger NO₂ in the middle and upper troposphere. The change in AMF is -56.0% over urban areas and 44.9-32.0% over rural areas; the corresponding change in AMF is -56.0% and -32.0% VCD increases by 134.9% and 44.9%, respectively. In contrast, Aug 24 is an example where the lightning parameterization has very little effect. The While the positive bias in NO₂ aloft is also observed by using G3/CTH parameterization, the amount of NO₂ in the middle and upper troposphere is smaller than Sep 10. It leads to lower sensitivity in AMF to the erroneous NO₂ caused by the lightning parameterization. With smaller relative change in AMF, the relative change in VCD is 3.1% over urban areas and -4.6% over rural areas.

4 Discussion

Here, we apply the improved KF/CAPE-PR simulation to the problem of constraining LNO_x production over CONUS. To do so, we vary the lightning NO_x production rate prescribed in WRF-Chem to produce the simulated map of NO₂ VCD, and compare against OMI NO₂ retrievals using a priori profiles from model simulations with the same LNO_x production rate. In our model-satellite comparisons the averaging kernel is applied to remove the representative errors introduced by a priori knowledges of NO₂ vertical profiles (Boersma et al., 2016). Figure 4 shows the difference between satellite retrieved NO₂ VCD and model simulated NO₂ VCD without lightning NO_x (a) and with lightning NO_x production rate of 500 mol NO flash⁻¹ (b) averaged between May 13 to June 23, 2012. Figure S4 shows difference plots with varied lightning NO_x production rates (400 and 665 mol NO flash⁻¹). The corresponding root-mean-square errors (RMSE) are included in Table S1. LNO_x production rate of 500 mol NO flash⁻¹ yields the lowest RMSE of 0.41×10^{15} mole cm⁻² between modeled and observed NO₂ VCD over CONUS. This is at the high end of previous estimates of the lightning NO_x production rate (16-700 mol NO flash⁻¹).

The RMSE for urban areas (top 5% of NO₂ VCD simulated by WRF-Chem without LNO_x) remains at high value (~0.9-1.3×10¹⁵ mole cm⁻²) when switching the LNO_x production rate. It indicates that the bias in the modeled VCD over urban areas is more likely due to surface NO₂. The RMSE for non-urban areas shows pronounced change with varied LNO_x production rate. Excluding urban areas lowers the RMSE to 0.37×10^{15} mole cm⁻² for LNO_x production rate of 500 mol NO flash⁻¹. The RMSEs are significant considering the uncertainty for retrievals. During the average time period, 32 ± 6 pixels contribute to each value in the plots. While the global mean uncertainty for tropospheric NO₂ VCD retrievals is 1×10^{15} mole

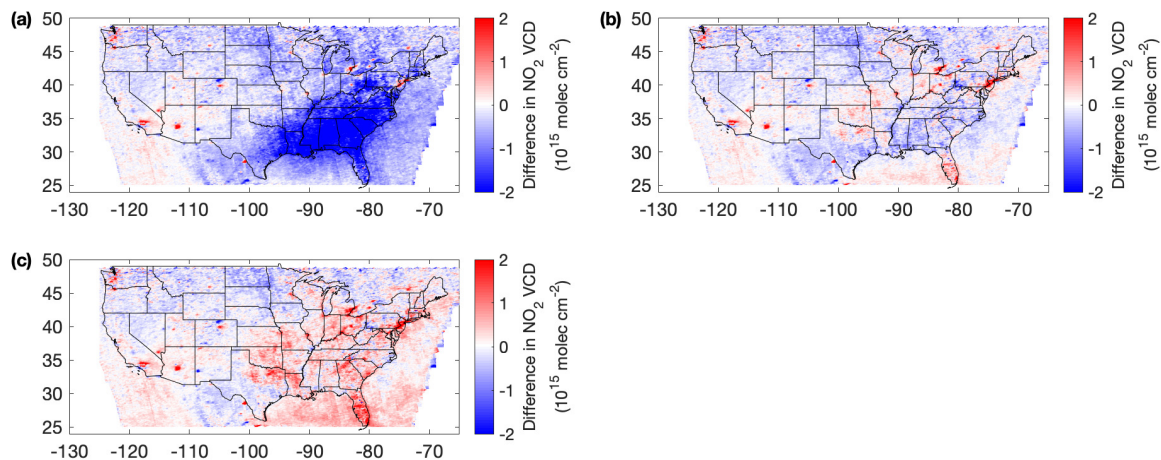


Figure 4. Difference in NO_2 VCD between BEHR retrievals and WRF-Chem (“WRF-Chem” – “BEHR”). (a) excludes LNO_x in model simulation, (b) adds LNO_x emission with production rate of $500 \text{ mol NO flash}^{-1}$. (c) includes the same LNO_x emission as (b) but uses NO_2 profiles scaled upward by 60% at pressure lower than 400 hPa. The average time covers May 13 to June 23, 2012. Pixels with cloud fraction larger than 0.2 are filtered out in the analysis.

cm^{-2} (Bucsela et al., 2013), the reduced uncertainty in our analysis is $\sim 0.2 \times 10^{15} \text{ mole cm}^{-2}$. The calculated RMSEs are twice of the uncertainty.

However, we note that this lightning NO_x estimate is systematically biased high due to the negative bias in $[\text{NO}_2]/[\text{NO}_x]$ ratio in the middle and upper troposphere. The satellite observed NO_2 column serves as a proxy for total NO_x emitted by lightning. The rapid interconversion between NO and NO_2 reaches the photochemical steady state in a short time ($\sim 120\text{s}$). Consequently, if the model kinetics result in an incorrect NO-NO_2 photochemical steady state ratio, this error will propagate into the LNO_x production estimate. Comparisons against aircraft measurements show $[\text{NO}_2]/[\text{NO}_x]$ ratio in the WRF-Chem simulations is around 40% smaller than observations in upper troposphere (Fig. S5). Given that the simulated $[\text{NO}_2]/[\text{NO}_x]$ is too small, the model will simulate smaller NO_2 VCDs per unit of LNO_x emitted, requiring a greater LNO_x production efficiency to match satellite NO_2 VCD observations. Comparison of modeled NO_2 columns recalculated with NO_2 profiles scaled up by 60% (the ratio of observed and modeled $[\text{NO}_2]/[\text{NO}_x]$) at pressure levels where $p < 400 \text{ hPa}$ and observations is shown in Fig. 4 (c). This suggests that the $500 \text{ mol NO flash}^{-1}$ is greater than the actual LNO_x production rate when the bias caused by $[\text{NO}_2]/[\text{NO}_x]$ ratio is accounted for.

Several recent studies also report an underestimate in modeled $[\text{NO}_2]/[\text{NO}_x]$ ratios in SE US (Travis et al., 2016; Silvern et al., 2018); both feature observations from SEAC4RS field campaign to validate model simulations. Silvern et al. (2018) suggests the underestimate is either caused by an unknown labile NO_x reservoir species or error in reaction rate constant for the $\text{NO} + \text{O}_3$ reaction and NO_2 photolysis reaction. In contrast, Nault et al. (2017) utilizes measurements from DC3 field campaign and demonstrates a positive bias in modeled $[\text{NO}_2]/[\text{NO}_x]$ ratio compared against observations. Understanding the

difference in $[\text{NO}_2]/[\text{NO}_x]$ between model and observations requires additional study, but is crucial to reducing the uncertainty in LNO_x estimates.

5 Conclusions

- 5 We implement an alternative lightning parameterization based on convective available potential energy and precipitation rate into WRF-Chem and couple it with Kain Frisch convective scheme. We ~~evaluate its performance in simulating lightning.~~ We first validate it by comparing against lightning observations and ~~conclude that the KF/CAPE-PR parameterization with a regional scaling factor of 0.5~~ find that the switch of convective scheme reproduces day-to-day variation of lightning flashes in the southeastern US ~~improves the model representation of spatial pattern and day-to-day variation of lightning flashes.~~ and the switch of lightning parameterization contributes to the improvement on lightning representation elsewhere in the US. We also compare the simulated NO_2 profiles against aircraft measurements and find that the simulated NO_2 using KF/CAPE-PR is more consistent with observations in the mid and upper troposphere.
- 10

The improved lightning NO_2 simulation has significant impact on AMFs and VCD of NO_2 . Over the southeastern US the AMF is reduced by 16% on average leading to a 19% increase in the NO_2 VCD. The effects on AMF and on VCD are very locally dependent. The VCD increase over urban areas is more pronounced and can be up to over 100%. This study emphasizes the importance of including reliable lightning NO_2 in a priori profiles for satellite retrievals.

15

The model-satellite NO_2 column comparison suggests $500 \text{ mol NO flash}^{-1}$ is ~~too high~~ the upper bound for the estimate of lightning NO_x production rate, ~~but demonstrate that the uncertainty in the modeled UT /ratio is a key limiting factor in constraining production efficiency over CONUS in the far-field approaches.~~

- 20 *Data availability.* The experimental branch of BEHR v3.0B product used in this study is hosted by UC Dash (Zhu et al., 2019a, b) as well as on behr.cchem.berkeley.edu. The BEHR algorithm is available at <https://github.com/CohenBerkeleyLab/BEHR-core/> (Laughner and Zhu, 2018). The revised WRF-Chem code is available at <https://github.com/CohenBerkeleyLab/WRF-Chem-R2SMH/tree/lightning> (Zhu and Laughner, 2019).

Author contributions. RCC directed the research and QZ, JLL and RCC designed this study; JLL and QZ developed BEHR products; QZ performed the analysis and prepared the manuscript with contributions from JLL and RCC. All authors have reviewed and edited the paper.

25

Competing interests. The authors declare no competing interests.

Acknowledgements. This work was supported by a NASA ESS Fellowship NNX14AK89H (Laughner), NASA grants NNX15AE37G and 80NSSC18K0624, and the TEMPO project SV3-83019. We acknowledge use of the Savio computational cluster resource provided by the Berkeley Research Computing program at UC Berkeley which is supported by the UC Berkeley Chancellor, Vice Chancellor for Research, and Chief Information Officer. We thank Earth Networks Company for providing the Earth Networks Total Lightning Network (ENTLN) datasets. We appreciate use of the WRF-Chem preprocessor tool (mozbc) provided by the Atmospheric Chemistry Observations and Modeling Lab (ACOM) of NCAR and use of MOZART-4 global model output available at <http://www.acom.ucar.edu/wrfchem/mozart.shtml>.

References

- 5 Allen, D., Pickering, K., Duncan, B., and Damon, M.: Impact of lightning NO emissions on North American photochemistry as determined using the Global Modeling Initiative (GMI) model, *Journal of Geophysical Research: Atmospheres*, 115, <https://doi.org/10.1029/2010JD014062>, <https://agupubs.onlinelibrary.wiley.com/doi/abs/10.1029/2010JD014062>, 2010.
- Allen, D. J. and Pickering, K. E.: Evaluation of lightning flash rate parameterizations for use in a global chemical transport model, *J. Geophys. Res. Atmos.*, 107, ACH 15–1–ACH 15–21, <https://doi.org/10.1029/2002JD002066>, <https://agupubs.onlinelibrary.wiley.com/doi/abs/10.1029/2002JD002066>, 2002.
- 10 Barth, M. C., Cantrell, C. A., Brune, W. H., Rutledge, S. A., Crawford, J. H., Huntrieser, H., Carey, L. D., MacGorman, D., Weisman, M., Pickering, K. E., Bruning, E., Anderson, B., Apel, E., Biggerstaff, M., Campos, T., Campuzano-Jost, P., Cohen, R., Crouse, J., Day, D. A., Diskin, G., Flocke, F., Fried, A., Garland, C., Heikes, B., Honomichl, S., Hornbrook, R., Huey, L. G., Jimenez, J. L., Lang, T., Lichtenstern, M., Mikoviny, T., Nault, B., O'Sullivan, D., Pan, L. L., Peischl, J., Pollack, I., Richter, D., Riemer, D., Ryerson, T., Schlager, H., St. Clair, J., Walega, J., Weibring, P., Weinheimer, A., Wennberg, P., Wisthaler, A., Wooldridge, P. J., and Ziegler, C.: The Deep Convective Clouds and Chemistry (DC3) Field Campaign, *Bulletin of the American Meteorological Society*, 96, 1281–1309, <https://doi.org/10.1175/BAMS-D-13-00290.1>, <https://doi.org/10.1175/BAMS-D-13-00290.1>, 2015.
- 15 Beirle, S., Huntrieser, H., and Wagner, T.: Direct satellite observations of lightning-produced NO_x, *Atmos. Chem. Phys.*, 10, 10965–10986, <https://doi.org/10.5194/acp-10-10965-2010>, 2010.
- 20 Boccippio, D. J., Koshak, W. J., and Blakeslee, R. J.: Performance Assessment of the Optical Transient Detector and Lightning Imaging Sensor. Part I: Predicted Diurnal Variability, *Journal of Atmospheric and Oceanic Technology*, 19, 1318–1332, [https://doi.org/10.1175/1520-0426\(2002\)019<1318:PAOTOT>2.0.CO;2](https://doi.org/10.1175/1520-0426(2002)019<1318:PAOTOT>2.0.CO;2), [https://doi.org/10.1175/1520-0426\(2002\)019<1318:PAOTOT>2.0.CO;2](https://doi.org/10.1175/1520-0426(2002)019<1318:PAOTOT>2.0.CO;2), 2002.
- Boersma, K. F., Vinken, G. C. M., and Eskes, H. J.: Representativeness errors in comparing chemistry transport and chemistry climate models with satellite UV–Vis tropospheric column retrievals, *Geoscientific Model Development*, 9, 875–898, <https://doi.org/10.5194/gmd-9-875-2016>, <https://www.geosci-model-dev.net/9/875/2016/>, 2016.
- 25 Bucsela, E., Krotkov, N., Celarier, E., Lamsal, L., Swartz, W., Bhartia, P., Boersma, K., Veefkind, J., Gleason, J., and Pickering, K.: "A new tropospheric and stratospheric NO₂ retrieval algorithm for nadir-viewing satellite instruments: applications to OMI, *Atmos. Meas. Tech.*, 6, 2607–2626, <https://doi.org/10.5194/amt-6-2607-2013>, 2013.
- 30 Bucsela, E. J., Pickering, K. E., Huntemann, T. L., Cohen, R. C., Perring, A., Gleason, J. F., Blakeslee, R. J., Albrecht, R. I., Holzworth, R., Cipriani, J. P., Vargas-Navarro, D., Mora-Segura, I., Pacheco-Hernández, A., and Laporte-Molina, S.: Lightning-generated NO_x seen by the Ozone Monitoring Instrument during NASA's Tropical Composition, Cloud and Climate Coupling Experiment (TC4), *Journal of Geophysical Research: Atmospheres*, 115, n/a–n/a, <https://doi.org/10.1029/2009JD013118>, <http://dx.doi.org/10.1029/2009JD013118>, d00J10, 2010.
- 35 Cecil, D. J., Buechler, D. E., and Blakeslee, R. J.: Gridded lightning climatology from TRMM-LIS and OTD: Dataset description, *Atmospheric Research*, 135–136, 404 – 414, <https://doi.org/https://doi.org/10.1016/j.atmosres.2012.06.028>, <http://www.sciencedirect.com/science/article/pii/S0169809512002323>, 2014.
- Choi, Y., Wang, Y., Zeng, T., Martin, R. V., Kurosuo, T. P., and Chance, K.: Evidence of lightning NO_x and convective transport of pollutants in satellite observations over North America, *Geophysical Research Letters*, 32, <https://doi.org/10.1029/2004GL021436>, <https://agupubs.onlinelibrary.wiley.com/doi/abs/10.1029/2004GL021436>, 2005.

- Crutzen, P. J.: The Role of NO and NO₂ in the Chemistry of the Troposphere and Stratosphere, *Annual Review of Earth and Planetary Sciences*, 7, 443–472, <https://doi.org/10.1146/annurev.ea.07.050179.002303>, <https://doi.org/10.1146/annurev.ea.07.050179.002303>, 1979.
- 5 Cummings, K. A., Huntemann, T. L., Pickering, K. E., Barth, M. C., Skamarock, W. C., Höller, H., Betz, H.-D., Volz-Thomas, A., and Schlager, H.: Cloud-resolving chemistry simulation of a Hector thunderstorm, *Atmospheric Chemistry and Physics*, 13, 2757–2777, <https://doi.org/10.5194/acp-13-2757-2013>, <https://www.atmos-chem-phys.net/13/2757/2013/>, 2013.
- DeCaria, A. J., Pickering, K. E., Stenchikov, G. L., and Ott, L. E.: Lightning-generated NO_x and its impact on tropospheric ozone production: A three-dimensional modeling study of a Stratosphere-Troposphere Experiment: Radiation, Aerosols and Ozone (STRAO-A) thunderstorm, *Journal of Geophysical Research: Atmospheres*, 110, <https://doi.org/10.1029/2004JD005556>, <https://agupubs.onlinelibrary.wiley.com/doi/abs/10.1029/2004JD005556>, 2005.
- 10 Delmas, R., Serça, D., and Jambert, C.: Global inventory of NO_x sources, *Nutrient Cycling in Agroecosystems*, 48, 51–60, <https://doi.org/10.1023/A:1009793806086>, <https://doi.org/10.1023/A:1009793806086>, 1997.
- 15 Denman, K. L., Chidthaisong, A., Ciaia, P., Cox, P. M., Dickinson, R. E., Hauglustaine, D., Heinze, C., Holland, E., Lohmann, U., Rameshbabu, S., et al.: Couplings between changes in the climate system and biogeochemistry, *International Panel on Climate Change*, pp. 499–587, 2007.
- EPA: Air Pollutant Emissions Trends Data, <https://www.epa.gov/air-emissions-inventories/air-pollutant-emissions-trends-data>, 2016.
- Finney, D. L., Doherty, R. M., Wild, O., Huntrieser, H., Pumphrey, H. C., and Blyth, A. M.: Using cloud ice flux to parametrise large-scale lightning, *Atmospheric Chemistry and Physics*, 14, 12 665–12 682, <https://doi.org/10.5194/acp-14-12665-2014>, <https://www.atmos-chem-phys.net/14/12665/2014/>, 2014.
- 20 Grell, G. A.: Prognostic Evaluation of Assumptions Used by Cumulus Parameterizations, *Monthly Weather Review*, 121, 764–787, [https://doi.org/10.1175/1520-0493\(1993\)121<0764:PEOAUB>2.0.CO;2](https://doi.org/10.1175/1520-0493(1993)121<0764:PEOAUB>2.0.CO;2), [https://doi.org/10.1175/1520-0493\(1993\)121<0764:PEOAUB>2.0.CO;2](https://doi.org/10.1175/1520-0493(1993)121<0764:PEOAUB>2.0.CO;2), 1993.
- 25 Grell, G. A. and Dévényi, D.: A generalized approach to parameterizing convection combining ensemble and data assimilation techniques, *Geophysical Research Letters*, 29, 38–1–38–4, <https://doi.org/10.1029/2002GL015311>, <https://agupubs.onlinelibrary.wiley.com/doi/abs/10.1029/2002GL015311>, 2002.
- Guenther, A., Karl, T., Harley, P., Wiedinmyer, C., Palmer, P. I., and Geron, C.: Estimates of global terrestrial isoprene emissions using MEGAN (Model of Emissions of Gases and Aerosols from Nature), *Atmos. Chem. Phys.*, 6, 3181–3210, [https://doi.org/10.5194/acp-6-](https://doi.org/10.5194/acp-6-3181-2006)
- 30 [3181-2006](https://doi.org/10.5194/acp-6-3181-2006), <http://www.atmos-chem-phys.net/6/3181/2006/>, 2006.
- Hudman, R. C., Jacob, D. J., Turquety, S., Leibensperger, E. M., Murray, L. T., Wu, S., Gilliland, A. B., Avery, M., Bertram, T. H., Brune, W., Cohen, R. C., Dibb, J. E., Flocke, F. M., Fried, A., Holloway, J., Neuman, J. A., Orville, R., Perring, A., Ren, X., Sachse, G. W., Singh, H. B., Swanson, A., and Wooldridge, P. J.: Surface and lightning sources of nitrogen oxides over the United States: Magnitudes, chemical evolution, and outflow, *J. Geophys. Res. Atmos.*, 112, <https://doi.org/10.1029/2006JD007912>, 2007.
- 35 Huntrieser, H., Schlager, H., Lichtenstern, M., Roiger, A., Stock, P., Minikin, A., Höller, H., Schmidt, K., Betz, H.-D., Allen, G., Viciani, S., Ulanovsky, A., Ravegnani, F., and Brunner, D.: NO_x production by lightning in Hector: first airborne measurements during SCOUT-O3/ACTIVE, *Atmospheric Chemistry and Physics*, 9, 8377–8412, <https://doi.org/10.5194/acp-9-8377-2009>, <https://www.atmos-chem-phys.net/9/8377/2009/>, 2009.
- Jourdain, L., Kulawik, S. S., Worden, H. M., Pickering, K. E., Worden, J., and Thompson, A. M.: Lightning NO_x emissions over the USA constrained by TES ozone observations and the GEOS-Chem model, *Atmospheric Chemistry and Physics*, 10, 107–119, <https://doi.org/10.5194/acp-10-107-2010>, <https://www.atmos-chem-phys.net/10/107/2010/>, 2010.

- Kain, J. S.: The Kain–Fritsch Convective Parameterization: An Update, *Journal of Applied Meteorology*, 43, 170–181, [https://doi.org/10.1175/1520-0450\(2004\)043<0170:TKCPAU>2.0.CO;2](https://doi.org/10.1175/1520-0450(2004)043<0170:TKCPAU>2.0.CO;2), [https://doi.org/10.1175/1520-0450\(2004\)043<0170:TKCPAU>2.0.CO;2](https://doi.org/10.1175/1520-0450(2004)043<0170:TKCPAU>2.0.CO;2), 2004.
- Kain, J. S. and Fritsch, J. M.: A One-Dimensional Entraining/Detraining Plume Model and Its Application in Convective Parameterization, *Journal of the Atmospheric Sciences*, 47, 2784–2802, [https://doi.org/10.1175/1520-0469\(1990\)047<2784:AODEPM>2.0.CO;2](https://doi.org/10.1175/1520-0469(1990)047<2784:AODEPM>2.0.CO;2), [https://doi.org/10.1175/1520-0469\(1990\)047<2784:AODEPM>2.0.CO;2](https://doi.org/10.1175/1520-0469(1990)047<2784:AODEPM>2.0.CO;2), 1990.
- 10 Lamsal, L. N., Martin, R. V., Padmanabhan, A., van Donkelaar, A., Zhang, Q., Sioris, C. E., Chance, K., Kurosu, T. P., and Newchurch, M. J.: Application of satellite observations for timely updates to global anthropogenic NO_x emission inventories, *Geophysical Research Letters*, 38, n/a–n/a, <https://doi.org/10.1029/2010gl046476>, <https://doi.org/10.1029/2010gl046476>, 2011.
- Lapierre, J. L., Laughner, J. L., Geddes, J. A., Koshak, W., Cohen, R. C., and Pusede, S. E.: Observing regional variability in lightning NO_x production rates, in: *Journal of Geophysical Research*, submitted.
- 15 Laughner, J. L. and Cohen, R. C.: Quantification of the effect of modeled lightning NO₂ on UV–visible air mass factors, *Atmospheric Measurement Techniques*, 10, 4403–4419, <https://doi.org/10.5194/amt-10-4403-2017>, <https://www.atmos-meas-tech.net/10/4403/2017/>, 2017.
- Laughner, J. L. and Zhu, Q.: CohenBerkeleyLab/BEHR-Core: BEHR Core code, <https://doi.org/10.5f281/zenodo.998275>, 2018.
- Laughner, J. L., Zhu, Q., and Cohen, R. C.: The Berkeley High Resolution Tropospheric NO₂ Product, *Earth System Science Data Discussions*, 2018, 1–33, <https://doi.org/10.5194/essd-2018-66>, <https://www.earth-syst-sci-data-discuss.net/essd-2018-66/>, 2018.
- Laughner, J. L., Zhu, Q., and Cohen, R. C.: Evaluation of version 3.0B of the BEHR OMI NO₂ product, *Atmospheric Measurement Techniques*, 12, 129–146, <https://doi.org/10.5194/amt-12-129-2019>, <https://www.atmos-meas-tech.net/12/129/2019/>, 2019.
- Levelt, P., Oord, G., R. Dobber, M., Mälkki, A., Visser, H., Vries, J., Stammes, P., Lundell, J., and Saari, H.: The Ozone Monitoring Instrument, *IEEE T. Geoscience and Remote Sensing*, 44, 1093–1101, <https://doi.org/10.1109/TGRS.2006.872333>, 2006.
- 25 Liaskos, C. E., Allen, D. J., and Pickering, K. E.: Sensitivity of tropical tropospheric composition to lightning NO_x production as determined by replay simulations with GEOS-5, *Journal of Geophysical Research: Atmospheres*, 120, 8512–8534, <https://doi.org/10.1002/2014JD022987>, <https://agupubs.onlinelibrary.wiley.com/doi/abs/10.1002/2014JD022987>, 2015.
- Lu, Z., Streets, D. G., de Foy, B., Lamsal, L. N., Duncan, B. N., and Xing, J.: Emissions of nitrogen oxides from US urban areas: estimation from Ozone Monitoring Instrument retrievals for 2005–2014, *Atmospheric Chemistry and Physics*, 15, 10367–10383, <https://doi.org/10.5194/acp-15-10367-2015>, <https://www.atmos-chem-phys.net/15/10367/2015/>, 2015.
- 30 Luo, C., Wang, Y., and Koshak, W. J.: Development of a self-consistent lightning NO_x simulation in large-scale 3-D models, *Journal of Geophysical Research: Atmospheres*, 122, 3141–3154, <https://doi.org/10.1002/2016JD026225>, <https://agupubs.onlinelibrary.wiley.com/doi/abs/10.1002/2016JD026225>, 2017.
- Mak, H. W. L., Laughner, J. L., Fung, J. C. H., Zhu, Q., and Cohen, R. C.: Improved Satellite Retrieval of Tropospheric NO₂ Column Density via Updating of Air Mass Factor (AMF): Case Study of Southern China, *Remote Sensing*, 10, <http://www.mdpi.com/2072-4292/10/11/1789>, 2018.
- Martin, R., Sauvage, B., Folkens, I., Sioris, C., Boone, C., Bernath, P., and Ziemke, J.: Space-based constraints on the production of nitric oxide by lightning, *J. Geophys. Res. Atmos.*, 112, <https://doi.org/10.1029/2006JD007831>, 2007.
- Miyazaki, K., Eskes, H., and Sudo, K.: Global NO_x emissions estimates derived from an assimilation of OMI tropospheric NO₂ columns, *Atmos. Chem. Phys.*, 12, 2263–2288, <https://doi.org/10.5194/acp-12-2263-2012>, 2012.

- Miyazaki, K., Eskes, H., Sudo, K., and Zhang, C.: Global lightning NO_x production estimated by an assimilation of multiple satellite data sets, *Atmos. Chem. Phys.*, 14, 3277–3305, <https://doi.org/10.5194/acp-14-3277-2014>, 2014.
- 5 Nault, B. A., Laughner, J. L., Wooldridge, P. J., Crouse, J. D., Dibb, J., Diskin, G., Peischl, J., Podolske, J. R., Pollack, I. B., Ryerson, T. B., Scheuer, E., Wennberg, P. O., and Cohen, R. C.: Lightning NO_x Emissions: Reconciling Measured and Modeled Estimates With Updated NO_x Chemistry, *Geophys. Res. Lett.*, <https://doi.org/10.1002/2017GL074436>, 2017.
- Ott, L. E., Pickering, K. E., Stenchikov, G. L., Allen, D. J., DeCaria, A. J., Ridley, B., Lin, R.-F., Lang, S., and Tao, W.-K.: Production of lightning NO_x and its vertical distribution calculated from three-dimensional cloud-scale chemical transport model simulations, *Journal of Geophysical Research*, 115, <https://doi.org/10.1029/2009jd011880>, <https://doi.org/10.1029/2009jd011880>, 2010.
- 10 Pickering, K. E., Bucsel, E., Allen, D., Ring, A., Holzworth, R., and Krotkov, N.: Estimates of lightning NO_x production based on OMI NO₂ observations over the Gulf of Mexico, *J. Geophys. Res. Atmos.*, 121, 8668–8691, <https://doi.org/10.1002/2015JD024179>, <http://dx.doi.org/10.1002/2015JD024179>, 2015JD024179, 2016.
- 15 Pollack, I. B., Homeyer, C. R., Ryerson, T. B., Aikin, K. C., Peischl, J., Apel, E. C., Campos, T., Flocke, F., Hornbrook, R. S., Knapp, D. J., Montzka, D. D., Weinheimer, A. J., Riemer, D., Diskin, G., Sachse, G., Mikoviny, T., Wisthaler, A., Bruning, E., MacGorman, D., Cummings, K. A., Pickering, K. E., Huntrieser, H., Lichtenstern, M., Schlager, H., and Barth, M. C.: Airborne quantification of upper tropospheric NO_x production from lightning in deep convective storms over the United States Great Plains, *Journal of Geophysical Research: Atmospheres*, 121, 2002–2028, <https://doi.org/10.1002/2015JD023941>, <https://agupubs.onlinelibrary.wiley.com/doi/abs/10.1002/2015JD023941>, 2016.
- 20 Price, C. and Rind, D.: A simple lightning parameterization for calculating global lightning distributions, *Journal of Geophysical Research: Atmospheres*, 97, 9919–9933, <https://doi.org/10.1029/92JD00719>, <https://agupubs.onlinelibrary.wiley.com/doi/abs/10.1029/92JD00719>, 1992.
- Price, C., Penner, J., and Prather, M.: NO_x from lightning: 1. Global distribution based on lightning physics, *Journal of Geophysical Research: Atmospheres*, 102, 5929–5941, <https://doi.org/10.1029/96JD03504>, <https://agupubs.onlinelibrary.wiley.com/doi/abs/10.1029/96JD03504>, 1997.
- 25 Romps, D. M., Seeley, J. T., Vollaro, D., and Molinari, J.: Projected increase in lightning strikes in the United States due to global warming, *Science*, 346, 851–854, <https://doi.org/10.1126/science.1259100>, <http://science.sciencemag.org/content/346/6211/851>, 2014.
- Russell, A. R., Valin, L. C., and Cohen, R. C.: Trends in OMI NO₂ observations over the United States: effects of emission control technology and the economic recession, *Atmos. Chem. Phys.*, 12, 12 197–12 209, <https://doi.org/10.5194/acp-12-12197-2012>, 2012.
- 30 Schumann, U. and Huntrieser, H.: The global lightning-induced nitrogen oxides source, *Atmospheric Chemistry and Physics*, 7, 3823–3907, <https://doi.org/10.5194/acp-7-3823-2007>, <https://www.atmos-chem-phys.net/7/3823/2007/>, 2007.
- Silvern, R. F., Jacob, D. J., Travis, K. R., Sherwen, T., Evans, M. J., Cohen, R. C., Laughner, J. L., Hall, S. R., Ullmann, K., Crouse, J. D., Wennberg, P. O., Peischl, J., and Pollack, I. B.: Observed NO/NO₂ Ratios in the Upper Troposphere Imply Errors in NO-NO₂-O₃ Cycling Kinetics or an Unaccounted NO_x Reservoir, *Geophysical Research Letters*, 45, 4466–4474, <https://doi.org/10.1029/2018GL077728>, <https://agupubs.onlinelibrary.wiley.com/doi/abs/10.1029/2018GL077728>, 2018.
- 35 Tippet, M. K. and Koshak, W. J.: A Baseline for the Predictability of U.S. Cloud-to-Ground Lightning, *Geophysical Research Letters*, 0, <https://doi.org/10.1029/2018GL079750>, <https://agupubs.onlinelibrary.wiley.com/doi/abs/10.1029/2018GL079750>, 2018.
- Toon, O. B., Maring, H., Dibb, J., Ferrare, R., Jacob, D. J., Jensen, E. J., Luo, Z. J., Mace, G. G., Pan, L. L., Pfister, L., Rosenlof, K. H., Redemann, J., Reid, J. S., Singh, H. B., Thompson, A. M., Yokelson, R., Minnis, P., Chen, G., Jucks, K. W., and Pszenny, A.: Planning, implementation, and scientific goals of the Studies of Emissions and Atmospheric Composition, Clouds and Climate Coupling by Regional Sur-

- veys (SEAC4RS) field mission, *Journal of Geophysical Research: Atmospheres*, 121, 4967–5009, <https://doi.org/10.1002/2015JD024297>,
5 <https://agupubs.onlinelibrary.wiley.com/doi/abs/10.1002/2015JD024297>, 2016.
- Tost, H., Jöckel, P., and Lelieveld, J.: Lightning and convection parameterisations; uncertainties in global modelling, *Atmospheric Chemistry and Physics*, 7, 4553–4568, <https://doi.org/10.5194/acp-7-4553-2007>, <https://www.atmos-chem-phys.net/7/4553/2007/>, 2007.
- Travis, K. R., Jacob, D. J., Fisher, J. A., Kim, P. S., Marais, E. A., Zhu, L., Yu, K., Miller, C. C., Yantosca, R. M., Sulprizio, M. P., Thompson, A. M., Wennberg, P. O., Crouse, J. D., St. Clair, J. M., Cohen, R. C., Laughner, J. L., Dibb, J. E., Hall, S. R., Ullmann, K., Wolfe, G. M.,
10 Pollack, I. B., Peischl, J., Neuman, J. A., and Zhou, X.: Why do models overestimate surface ozone in the Southeast United States?, *Atmos. Chem. Phys.*, 16, 13 561–13 577, <https://doi.org/10.5194/acp-16-13561-2016>, <https://www.atmos-chem-phys.net/16/13561/2016/>, 2016.
- Wong, J., Barth, M. C., and Noone, D.: Evaluating a lightning parameterization based on cloud-top height for mesoscale numerical model simulations, *Geoscientific Model Development*, 6, 429–443, <https://doi.org/10.5194/gmd-6-429-2013>, <https://www.geosci-model-dev.net/6/429/2013/>, 2013.
- 15 Zare, A., Romer, P. S., Nguyen, T., Keutsch, F. N., Skog, K., and Cohen, R. C.: A comprehensive organic nitrate chemistry: insights into the lifetime of atmospheric organic nitrates, *Atmospheric Chemistry and Physics*, 18, 15 419–15 436, <https://doi.org/10.5194/acp-18-15419-2018>, <https://www.atmos-chem-phys.net/18/15419/2018/>, 2018.
- Zhao, C., Wang, Y., Choi, Y., and Zeng, T.: Summertime impact of convective transport and lightning NO_x production over North America: modeling dependence on meteorological simulations, *Atmospheric Chemistry and Physics*, 9, 4315–4327, <https://doi.org/10.5194/acp-9-4315-2009>, <https://www.atmos-chem-phys.net/9/4315/2009/>, 2009.
20
- Zhu, Q. and Laughner, J. L.: CohenBerkeleyLab/WRF-Chem-R2SMH: WRF-Chem code, <https://doi.org/10.5281/zenodo.2585381>, 2019.
- Zhu, Q., Laughner, J., and Cohen, R.: Berkeley High Resolution (BEHR) OMI NO₂ v3.0C - Gridded pixels, daily profiles, v3, UC Berkeley Dash, Dataset, <https://doi.org/10.6078/D16X1T>, 2019a.
- Zhu, Q., Laughner, J., and Cohen, R.: Berkeley High Resolution (BEHR) OMI NO₂ v3.0C - Native pixels, daily profiles, UC Berkeley Dash, Dataset, <https://doi.org/10.6078/D1BM2B>, 2019b.

Supplement to “Lightning NO₂ simulation over the Contiguous US and its effects on satellite NO₂ retrievals”

Qindan Zhu, Joshua L. Laughner and Ronald C. Cohen

S1 Comparison between ENTLN and NLDN

While both NLDN and ENTLN have high detection efficiency (>90%) for CG flashes, we recognize that ENTLN observes more CG flashes than NLDN. Shown in Fig. ??, we average the flashes density over CONUS both from ENTLN and NLDN between May 13 to June 23 2012. The daily averaged CG flash density from ENTLN is tightly correlated with those from NLDN with slope of 1.5. It can be explained by discrepancy in the grouping criterions applied to produce flash counts between NLDN and ENTLN. ENTLN groups all pulses within 10 km and 700 ms of each other as a single flash, and NLDN uses 10 km and 1000 ms as the threshold. In consequence, for the same amount of CG pulses measured by both lightning observation network, ENTLN produces more flashes than NLDN according to the grouping algorithm.

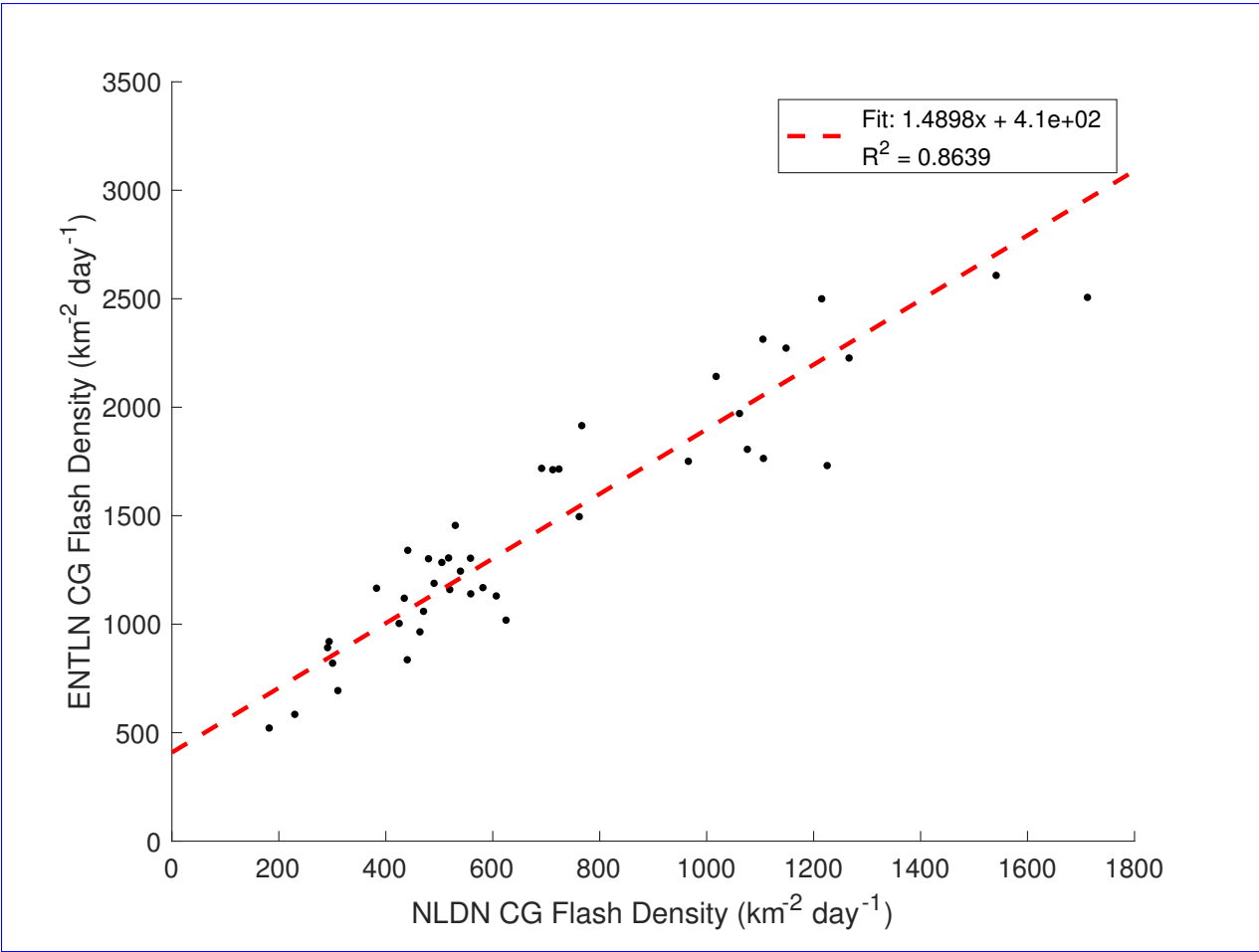


Figure S1: Comparison between CG flash density per day observed by NLDN and ENTLN. The data spans May 13 to June 23, 2012.

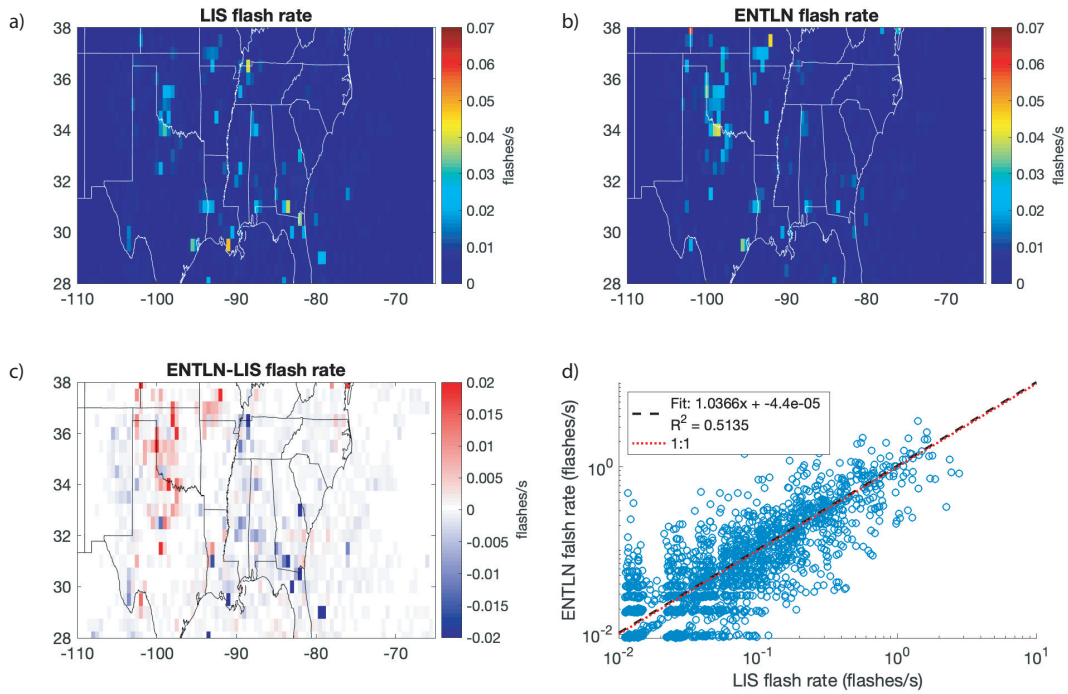


Figure S2: Comparison between flash rates observed by ENTLN and Lightning Imaging Sensor (LIS). ENTLN data is matched to corrected LIS flashes both in time and space during May 13-June 23, 2012, and both datasets are summed onto 0.5°x 0.5°grid spacing. (a,b) shows the spatial pattern of lightning flash rates measured by LIS (a) and ENTLN (b). The plot region covers 20°N - 38°N and 130°W - 65°W. (c,d) are corresponding absolute difference and scatter plots between LIS and ENTLN. LIS data is corrected using the detection efficiency from citetcecil14.

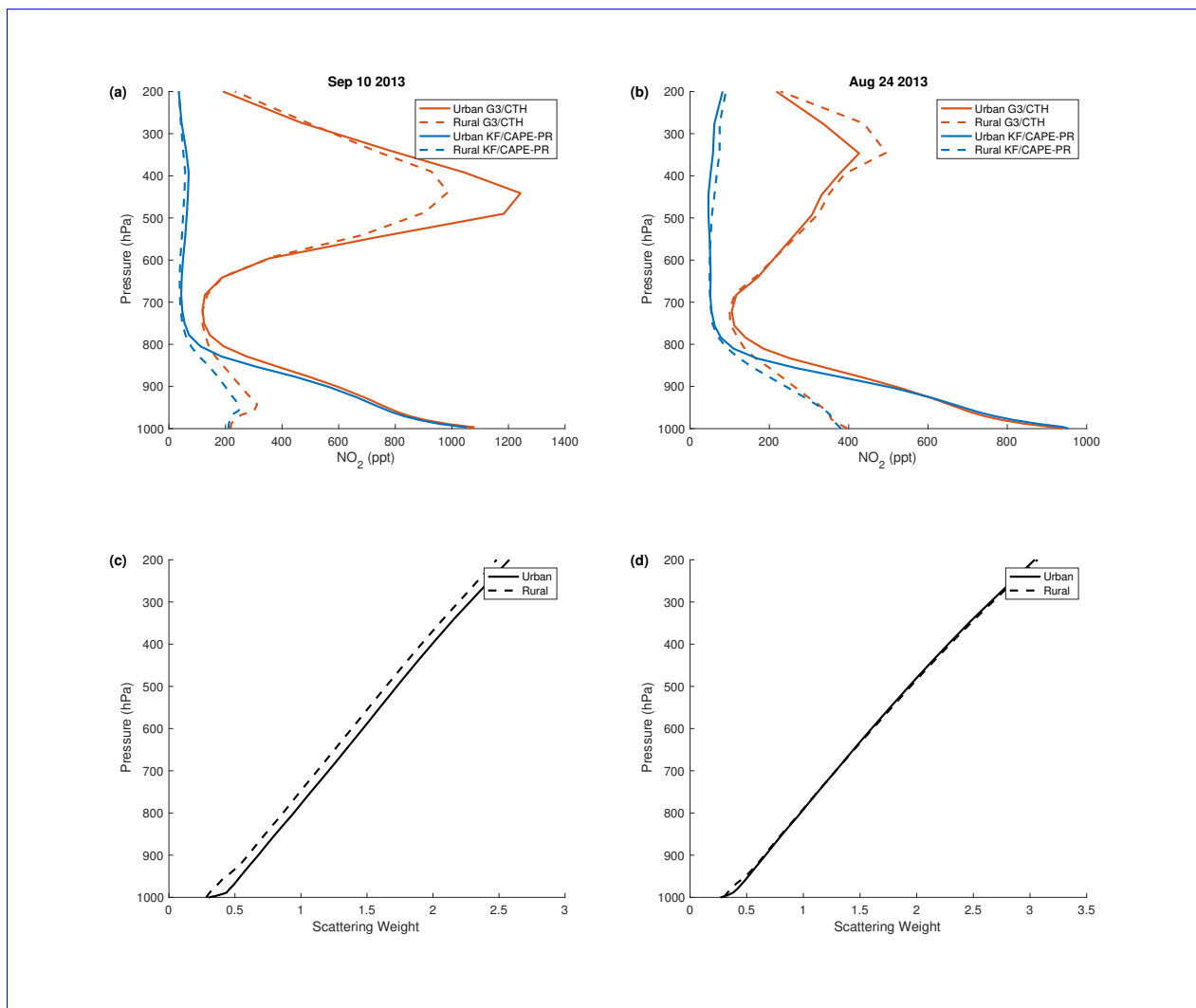


Figure S3: The a priori NO₂ vertical profiles (a, b) and scattering weights (c, d) on Sep 10 and Aug 24 2013 over urban and rural areas in SE US. The NO₂ profiles from WRF-Chem using G3/CTH parameterization are in red, those from KF/CAPE-PR parameterization are in blue.

| | No lightning | 400 mol NO $flash^{-1}$ | 500 mol NO $flash^{-1}$ | 665 mol NO $flash^{-1}$ |
|-----------|-----------------------|-------------------------|-------------------------|-------------------------|
| CONUS | 0.92×10^{15} | 0.44×10^{15} | 0.41×10^{15} | 0.44×10^{15} |
| Urban | 1.30×10^{15} | 0.89×10^{15} | 0.91×10^{15} | 1.10×10^{15} |
| Non-Urban | 0.90×10^{15} | 0.41×10^{15} | 0.37×10^{15} | 0.39×10^{15} |

Table S1: The root-mean-square errors (RMSE) in unit of mole cm^{-2} between observed and modeled NO_2 VCD using WRF-Chem with varied LNO_x production rates (0, 400, 500, 665 mol NO $flash^{-1}$). Urban areas are selected where NO_2 columns are at top 5% calculated from WRF-Chem without lightning. Non-urban areas are CONUS excluding urban areas.

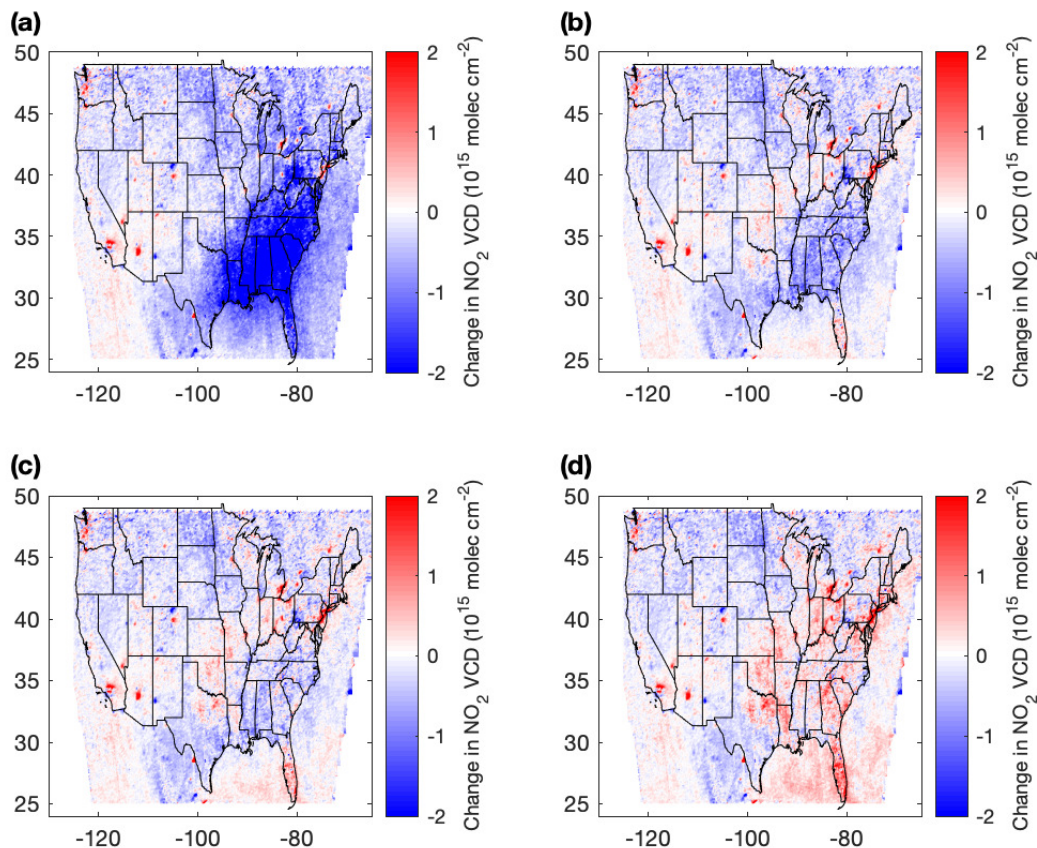


Figure S4: Difference in NO_2 VCD between BEHR retrievals and WRF-Chem (a) without LNO_x and with LNO_x production rate of (b) 400 mol NO $flash^{-1}$, (c) 500 mol NO $flash^{-1}$ and (d) 665 mol NO $flash^{-1}$.

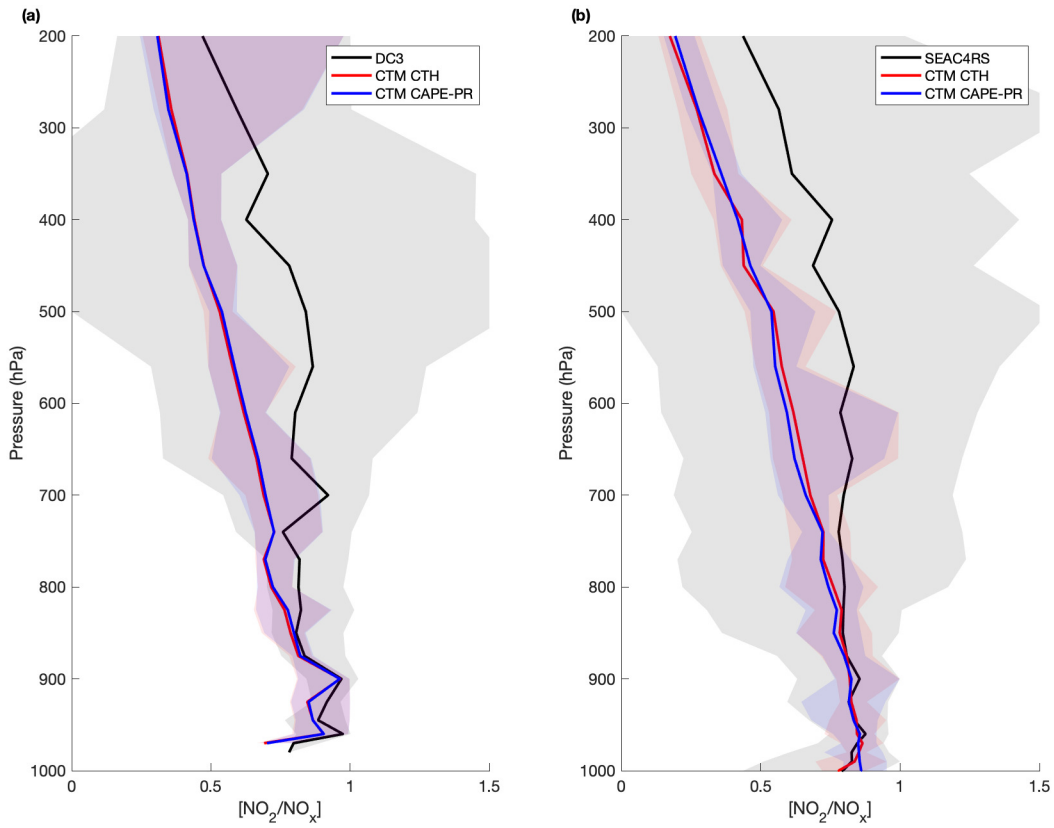


Figure S5: Comparison of WRF-Chem and aircraft $[NO_2/NO_x]$ profiles from the (a) DC3, (b) SEAC4RS campaigns. The solid line is the median of all profiles and the shaded areas are between 10th and 90th percentiles for each binned level. Aircraft measurements are shown in black, WRF-Chem using CTH lightning parameterization in red and WRF-Chem using CAPE-PR lightning parameterization in blue.